MEDCO

Modelling Engineering & Development Company Limited

Tubing Analysis System

TAS

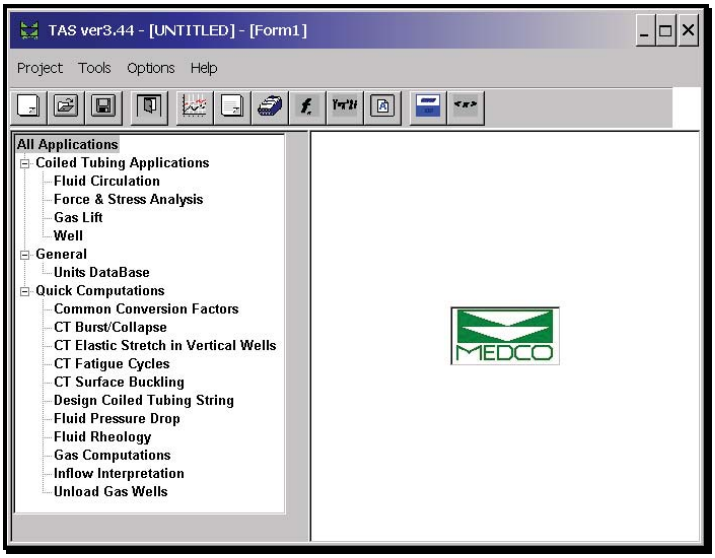

Technical Reference Manual

Courtenay House, Monument Way East, Woking, Surrey GU21 5LY, U.K.
Tel: +44-1483 750600 Fax: +44-1483 762233
Email: support@medcotas.com
Home Page: http://www.medcotas.com

Contents

1. INTRODUCTION AND HISTORICAL REMARKS 3

1.1 First Coiled Tubing Usage 3
1.2 Coiled Tubing Drilling – Tools and Equipment 3

2. FORCE AND STRESS ANALYSIS 6

2.1 The Boundary Condition 6
2.2 Tension Increment 8
2.3 Friction Factor 10
2.4 Fluid Drag 10
2.5 Buoyancy 11
2.6 Cable and Capillary Tubes 12
2.7 Stresses 13
2.8 Stability of Well Tubulars 14
2.9 Buckling 16
2.10 Bending Stress 17
2.11 Lockup 17
2.12 Weight on Bit (WOB) 20
2.13 Maximum Weight on Bit 21
2.14 Maximum Over Pull 22
2.15 Nomenclature 22
2.16 References 23

3. FATIGUE ANALYSIS 24

3.1 Effect of Equipment Size 25
3.2 Effects of Axial Stress on Fatigue Life 25
3.3 Effects of Pressure 27
3.4 Effects of Weight 28
3.5 Other Effects 28
3.6 Nomenclature 29
3.7 References 30

4. FLUID CIRCULATION 31

4.1 Single Phase Flow 31
4.2 Fluid Circulation Computations 33
4.3 Multi Phase Flow 34
4.4 Foam Flow 38
4.5 Pressure Losses in Multi Phase Flow 39
4.6 Cuttings Transport 47
4.7 Maximum Penetration Rate 49
4.8 Under-Balanced Drilling 50
4.9 Reservoir Production 50
4.10 Nomenclature 51
4.11 References 52

APPENDIX 53

1. INTRODUCTION AND HISTORICAL REMARKS

1.1 First Coiled Tubing Usage

Coiled tubing was first used to lay a pipeline, 83 kms long and 4" in diameter, between England and France during World WAR II. This project was known as project *PLUTO* and the full length of the tube was put on a floating drum. The process of laying the pipeline on the seabed took place over night.

The oil and gas industry first used coiled tubing to service wells in the early 1960's. But coiled tubing services were not immediately popular in the oilfields because of lack of confidence in its reliability. Many accidents that took place did not help build the confidence needed. The earlier coiled tubing manufacturing techniques did not help build reliable coiled tubing, also the sizes that were available were too small thus reducing its applications.

Enhanced production techniques and the introduction of larger coiled tubing sizes improved the reliability of the services and expanded its applications. The 1980's saw a rapid growth of the coiled tubing services and this growth has been sustained to date.

Services similar to coiled tubing drilling, in principle, were used well before the first coiled tubing drilling job. These services included under-reaming and milling where a downhole motor is used to turn a reamer to drill through debris or obstacles in the well. Coiled tubing drilling, though, requires more control of the coiled tubing to enable control of the trajectory of the well. New downhole tools and further advances in the coiled tubing made coiled tubing drilling possible.

1.2 Coiled Tubing Drilling – Tools and Equipment

To be able to drill a well, subject to a pre-planned trajectory, using coiled tubing instead of drill pipe several downhole tools are required.

- **Drill Bit;** This is required to drill the formation. Conventional small drill bits are suitable.

- **Downhole Motor;** This is required to turn the drill bit. Note that it is not possible to turn the coiled tubing string while the coiled tubing reel is stationary. Ideas of placing the reel on a large rotating table are currently being pursued by Transocean/Ensign Drilling[#]. As stated earlier, downhole motors have been available a long time.
- **Steering Tool;** This is a vital tool that allows control of the direction of drilling. The direction of drilling will determine both the deviation and azimuth of the well.

[#] For the purpose of this guide, the reel on a large rotating table will not be considered.

Most steering tools used today are operated hydraulically, requiring two capillary tubes to operate.

- **Measurement While Drilling (MWD);** MWD's can consist of several sensors. In drill pipe applications the MWD's are wireless and transmit their readings on the drilling mud. Wireless MWD's require a minimum flow of mud, normally not possible with coiled tubing because of the size constraint and the physical limitation of the burst pressure. In coiled tubing drilling, the MWD's are connected by a wireline to surface. The wireline supplies the necessary power to these tools and is used for transmitting their signals back to surface.

A basic combination of MWD's that is normally used in coiled tubing drilling consists of;

- **Deviation and Azimuth;** These readings are vital for the driller to enable real time control of the direction of the well. Deviation is measured using an accelerometer and azimuth using a magnetometer.

- **Vibrations;** This indicates to the driller whether the drill motor is still functioning or has stalled. Applying too much weight on bit can cause the motor to stall. The vibration tool normally gives an indication of the activities taking place at the bottom of the well but is not used for quantitative analysis.

- **Gamma Ray, Temperature Sub, Pressure Sub etc…;** Such tools are beyond the basic configuration required. These tools provide additional useful information such as depth correlation, bottom hole temperatures and pressure, and these can be used to ensure under-balanced or over-balanced drilling conditions. Other tools could be included, and no doubt in the future we will see more of these being added, and can consist of a Production Logging, Induction Resistivity, and many other logging tools. These, however, are of more use to geologists and reservoir engineers who may be able to make real time changes in the well plan.

As seen from the list of necessary tools, a wireline and capillary tubes are required to enable coiled tubing drilling to be carried out. When the first wirelines were installed inside coiled tubing (for coiled tubing logging), these were accompanied by several problems. The first problem is how to install a wireline in the coiled tubing then how to maintain a good connection between the wireline and the downhole tools. Fortunately, all of these problems are now well understood and applicable solutions have been adapted. The same problems and solutions apply equally to the capillary tubes.

New tools and techniques are continuously being looked at and developed. Some of the more interesting of these include;

- **Torque and Drag Measuring Sub**; the use of this tool will give an indication of the weight-on-bit and torque being applied.

- **Project Helix**; the basic idea of this project is to remove the cable and the capillaries. Instead, the fluid flow will be used to generate electrical power downhole, then electrically drive the various tools combination. Communication between the downhole tools and surface will be via the drilling fluid. Such an idea, if successfully implemented, would have great advantages because it will make the coiled tubing lighter thus less susceptible to buckling, and will allow a larger flow area to be available for the fluids, making higher flow rates achievable. There is also a commercial advantage to this idea. Currently, Cudd Pressure Control has a patent on Coiled Tubing Drilling with a Wireline inside. Although this patent has not deterred others from using this technique, it could stir up some legal problems in future.

2. FORCE AND STRESS ANALYSIS

In computing the forces that act upon coiled tubing, or any well tubular, we need to consider the weight of the tubular, the buoyancy, and any friction. Pressure forces also have a significant effect as they do exert an end force on the tubular. In addition, when fluid flow is significant the fluid drag must be considered.

When the coiled tubing is at a given depth the weight of the coiled tubing string, including the bottom hole assembly (BHA), can be computed by first considering the end force at the bottom of the coiled tubing (boundary condition), then computing tension increments per segment. The final tension computed will be that of the coiled tubing at surface and will represent the weight of the string at the given depth. When simulating a running-in or pulling out weight prediction, this procedure is repeated per individual depth station.

2.1 The Boundary Condition

Every coiled tubing drilling operation will involve some bottom hole assembly. By assuming that the BHA is short enough we can neglect the effects of any hydrostatic pressure difference between the bottom and top ends of the BHA. Also, this assumption allows us to neglect any fluid drag forces and buckling considerations regarding the BHA.

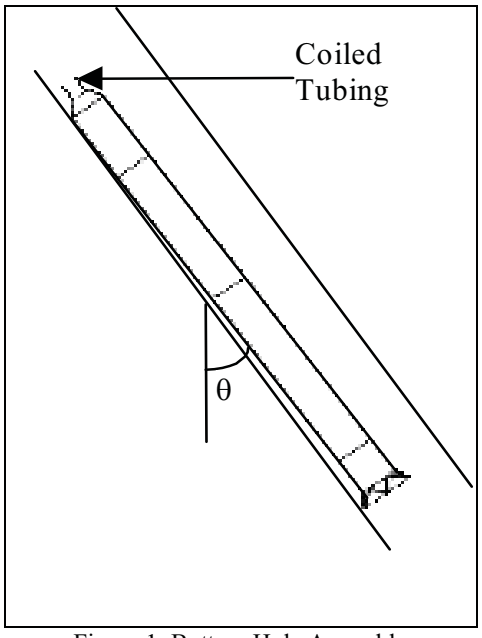

Figure 1: Bottom Hole Assembly

The boundary condition is, therefore, determined by an end force given as follows;

$$F_{end} = W_{bha} \cos\theta - P_o \frac{\pi}{4} d_o^2 + P_i \frac{\pi}{4} d_i^2 \pm Friction_{bha}$$

... 1

where W_{bha} is the buoyed weight of BHA
θ is the deviation
P_o is the pressure in the well
P_i is the internal coiled tubing pressure
d_o is the coiled tubing outer diameter
d_i is the coiled tubing inner diameter
and $Friction_{bha}$ is the friction force on the BHA

The buoyed weight of the BHA is given by;

$$W_{bha} = Wt_{bha} - V_{bha} * \rho_o$$

... 2

where Wt_{bha} is the weight of BHA,
V_{bha} is the volume of BHA,
and ρ_o is the density of the fluid in the well

while the friction force is given by;

$$Friction_{bha} = \mu W_{bha} \sin\theta$$

... 3

where μ is the friction factor

The friction force will be in the opposite direction to motion, thus, when running into the well the friction force will take the negative sign and vice versa. The end force, F_{end}, is the tension/compression that the coiled tubing will experience at the bottom.

The terms $P_o \frac{\pi}{4} d_o^2$ and $P_i \frac{\pi}{4} d_i^2$ in equation (1) represent the forces due to external and internal pressures respectively. Note that because of the fact that a BHA represents a restriction to the fluid flow, the internal pressure at the top of the BHA will be different from the external pressure at the bottom of the BHA. Thus the pressures will act on the respective cross sectional areas and exert a force. More details of the pressure computations are included in Chapter 4, “Fluid Circulation”.

While the internal pressure does represent a real force that acts to push the bottom end of the coiled tubing downwards, the internal coiled tubing pressure at

surface will also act upwards to lift the coiled tubing . When the coiled tubing is very close to surface, any increase in the internal pressure will not be reflected on the weight indicator as the upward force will negate the downward force. But the force does exist and must be taken into consideration in computing tension/compression and stresses. In figure 2, if the coiled tubing internal pressure at the top of the BHA was P_i, the internal area A_i, and the density of the fluid inside ρ_i, then the downward force will be P_iA_i and at the top of the injector, the internal pressure will be exerting an upward force $(P_i - \rho_I gz) A_i$. If the height z was small enough, then the upward and downward forces will be approximately equal.

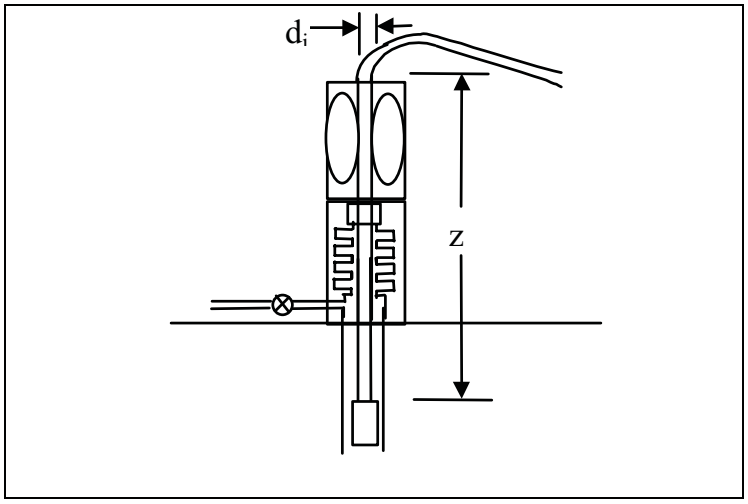

Figure 2: The effects of coiled tubing internal pressure

2.2 Tension Increment

In figure 3, let's assume the deviation and azimuth to be θ and ϕ at the bottom and $\theta + \Delta\theta$ and $\phi + \Delta\phi$ at the top, respectively. The tension increment then can be written as;

$$\Delta T = W \cos\bar{\theta} \pm \mu F_N \qquad \text{... 4}$$

Where $W \cos\bar{\theta}$ represents the axial buoyed weight component,
$\bar{\theta}$ represents the average deviation of the segment.
and μF_N represents the friction force.

The friction force is always in the opposite direction to motion. That is, when the coiled tubing is moving down, the sign of the last term in equation (4) will be negative and vice versa.

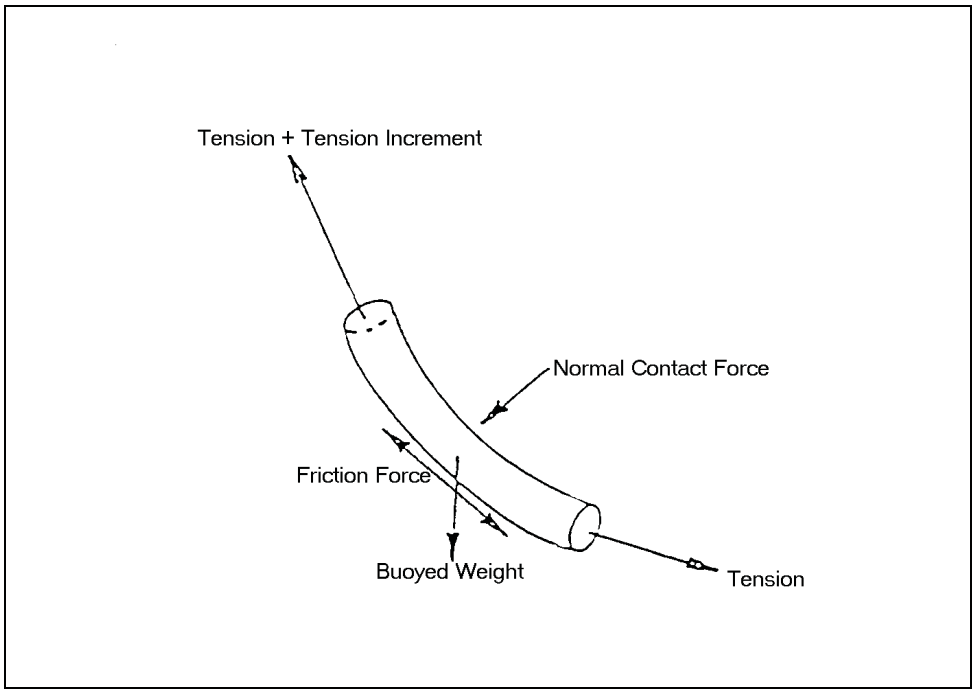

Figure 3: Forces acting on a coiled tubing segment in a deviated well

The normal force for a short segment of the coiled tubing is given by[1];

$$F_N = \sqrt{\left(T\Delta\phi \sin\bar{\theta}\right)^2 + \left(T\Delta\theta + W\sin\bar{\theta}\right)^2}$$

... 5

Equation (5) automatically takes care of whether the coiled tubing is on the lower or upper side of the well. Note that in our convention, and with reference to figure 3, $\Delta\theta$ is negative (the deviation at the lower end is greater than at the upper end). Also, T is positive when the coiled tubing is in tension and negative when in compression. Thus, when the coiled tubing is in tension, the component of the normal force due to tension, $T\Delta\theta$, is acting in the opposite direction to that of the weight, $W\sin\bar{\theta}$. This is expected since the tension will be pulling the coiled tubing towards the upper side of the well. The opposite is true when the coiled tubing is in compression.

By back substituting (5) in (4), we obtain an explicit expression for the tension increment. The tension at the top of the coiled tubing segment can now be computed and the tension at the bottom of the next coiled tubing segment will become known. This process is repeated until the final segment whose top is at surface. The tension at the top of the surface segment of coiled tubing will represent the weight of the coiled tubing at the particular depth being considered.

The weight reading as seen by the weight indicator, though, will include the effect of the stuffing box drag and the upward force due to internal pressure. The stuffing box drag is a friction force and, therefore, will be in the opposite direction to

motion. There is no known method of computing the stuffing box drag, as this force is a function of several parameters, some of which are unknown, that include the well head pressure and the state of the stripper rubber. Even during the same coiled tubing run, the state of the stripper rubber will vary, thus, changing the friction factor between the stripper and the coiled tubing. The stuffing box drag is estimated by the coiled tubing operator either from experience or, when very close to surface, taking half the difference between the pulling out and running in weights.

2.3 Friction Factor

Friction is a force that opposes the motion of coiled tubing and is a result of the interaction between surfaces in contact with each other. The friction force is proportional to the normal force between the surfaces, and the constant of proportionality is called the friction factor. The friction factor will vary depending on the surface roughness.

The normal force is computed using the expression in equation (5) above. An additional component due to buckling is also considered. The additional normal contact force due to buckling will be discussed later in this chapter when considering buckling of the coiled tubing.

The friction factor, also known as the Coefficient of Friction, is normally estimated from experience or by laboratory measurements. Some experiments were conducted to compute the friction factor between coiled tubing and casing resulting in a friction factor ranging between 0.20 and 0.25. In cases of bare foot completions or scale build-up, the friction factor is increased to 0.3 or even higher to 0.35.

It is difficult to assign a particular value to the friction factor for the cases of bare foot completions and scale build-up. However, a trial and error technique to match the weight readouts can be used to estimate the friction factor.

Experience from the Middle East and in particular formations indicated that an appropriate friction factor for open hole would be between 0.27 and 0.30 in limestone formation and between 0.29 and 0.32 in sandstone formation.

2.4 Fluid Drag

When significant fluid flow past the coiled tubing is encountered either through well production or pumped fluids, the fluid drag force must be considered. The fluid drag is caused by the shear stress of the fluid at the surface of the coiled tubing. The fluid drag force, ***D***, can be expressed as follows;

$$D = \frac{1}{2} C_D \rho_o S V^2$$

... 6

where C_D is the drag coefficient,
S is the surface area of the coiled tubing affected by the fluid flow,
and V is the relative velocity between the fluid and the coiled tubing.

The drag coefficient will vary depending on the flow regime, i.e. laminar, transitional, or turbulent flow. The flow regime is determined by computing the Reynolds number, ***Re***, defined as the ratio of inertia to viscous forces, and is given by;

$$\mathrm{Re} = \frac{\rho_o V d_o}{\eta} \qquad \text{... 7}$$

where η is the fluid viscosity. The flow is laminar for Reynolds numbers of 0 to 2,000 and turbulent beyond 10,000. Transitional flow exists between the two regimes.

In most coiled tubing applications, including drilling, this force is not significant enough and can be neglected particularly if the flow regime is laminar or transitional. The coefficient of drag is given by;

$$C_D = 0.074\,\mathrm{Re}^{-1/5} \text{ for Reynolds number up to } 10^7$$

$$C_D = \frac{0.455}{(\log_{10}\mathrm{Re})^{2.58}} \text{ for Reynolds number above } 10^7$$

Note that equation (6) can be used to determine the drag force per segment of the coiled tubing being considered, where the surface area will be that of the whole segment. Also, the fluid drag will be acting in the direction of the flow. Therefore, we can modify the tension increment expression in (4) to account for this drag force,

$$\Delta T = W\cos\bar{\theta} \pm \mu F_N - D \qquad \text{... 8}$$

The relative velocity between the fluid and the coiled tubing is considered positive when the flow is upwards.

2.5 Buoyancy

When an object is immersed in a fluid, the fluid exerts an upward force called buoyancy. This force is due to the hydrostatic pressure difference between the lower and upper surfaces of the object. Thus, in a vertical well, buoyancy is concentrated at the bottom of the coiled tubing, while, in a horizontal well, it is distributed along the length of the coiled tubing. In a deviated section, the

buoyancy is both concentrated and distributed. The buoyed weight of a coiled tubing segment is, therefore, given as;

$$W = Wt - \rho_o \frac{\pi}{4} d_o^2 \sin\bar{\theta} + \rho_i \frac{\pi}{4} d_i^2 \sin\bar{\theta}$$

... 9

where ρ_i is the density of the fluid inside the coiled tubing. Note that we already accounted for the concentrated buoyancy at the bottom of the coiled tubing when we derived the end force. Equation (9) accounts the remaining distributed buoyancy.

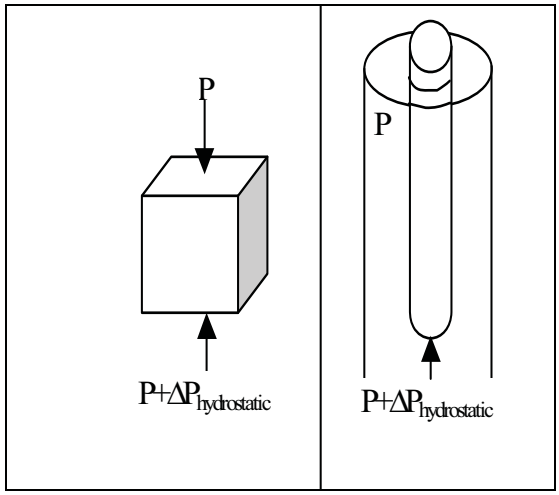

Figure 4: (a) Buoyancy is due to hydrostatic pressure difference, (b) Buoyancy on coiled tubing is concentrated at the bottom

2.6 Cable and Capillary Tubes

As mentioned previously, current coiled tubing drilling normally involves the use of a cable and two capillaries. The cable and the capillaries are only attached to the coiled tubing at two points, the first being a surface connection at the rotating end on the reel and the other is downhole at the top of the BHA. Because of the fact that the coiled tubing normally travels over a gooseneck which is in turn supported by a separate frame to that of the injector, the cables and capillaries weights will not be felt by the coiled tubing in a vertical well. Also these weights will not manifest themselves on the weight indicator. Mathematically, the weight of the cable and the capillaries can be included in the weight expression in the same way the buoyancy was included. Modifying equation (9) to include the weight of the cable and capillaries gives;

$$W = Wt - \rho_o \frac{\pi}{4} d_o^2 \sin\bar{\theta} + \rho_i \frac{\pi}{4} (d_i^2 - d_c^2) \sin\bar{\theta} + (W_c - \rho_i \frac{\pi}{4} d_c^2) \sin\bar{\theta}$$

... 10

where d_c represents the effective combined diameter of the cable and capillaries, and W_c represent the combined weight per unit length. The effective combined diameter can be computed as $d_c = \sqrt{d_{cable}^2 + n d_{capillary}^2}$,where n is the number of capillaries.

2.7 Stresses

Three components of stress act on the coiled tubing. The resultant stress is known as the tri-axial stress. The oil and gas industry favours the maximum distortion-energy theory for calculating tri-axial stresses in tubular goods. This is also known as the Von Mises relationship. The components of tri-axial stress are;

- **Axial Stress**

  The axial stress is the stress component due to axial force, i.e. tension or compression. The axial stress, σ_a , is given by;

$$\sigma_a = \frac{T}{\frac{\pi}{4}\left(d_o^2 - d_i^2\right)}$$

... 11

- **Hoop (Circumferential) and Radial Stresses**

  Both of these stress components are due to pressure forces. The hoop stress, σ_h, is given by[2];

$$\sigma_h = -\left[\frac{P_i r_i^2 - P_o r_o^2}{r_o^2 - r_i^2}\right] - \left[\frac{P_i - P_o}{r_o^2 - r_i^2}\right]\left[\frac{r_o^2 r_i^2}{r_d^2}\right]$$

... 12

while the radial stress, σ_r , is given by;

$$\sigma_r = -\left[\frac{P_i r_i^2 - P_o r_e^2}{r_o^2 - r_i^2}\right] + \left[\frac{P_i - P_o}{r_o^2 - r_i^2}\right]\left[\frac{r_o^2 r_i^2}{r_d^2}\right]$$

... 13

where r_i is the internal radius of the coiled tubing,
r_o is the outer radius of the coiled tubing,
and r_d is the radial distance to the point under consideration.

The Von Mises relationship gives the tri-axial stress as a function of the stress components;

$$2\sigma^2 = (\sigma_a - \sigma_r)^2 + (\sigma_r - \sigma_h)^2 + (\sigma_h - \sigma_a)^2$$

... 14

2.8 Stability of Well Tubulars

Buckling is a form of coiled tubing instability. To understand buckling, it first is necessary to understand stability. With reference to figure (5), if each ball is disturbed slightly from its position of equilibrium and then released: the ball in (a) returns to its original position, the ball in (b) remains in its new position, while the ball in (c) moves away from its original position until it reaches a new equilibrium. The ball in (a) is said to be stable, in (b) is in neutral stability, and in (c) is unstable. By examining the potential energy of the balls with reference to the surrounding, it can be seen that the higher the potential energy the higher the instability.

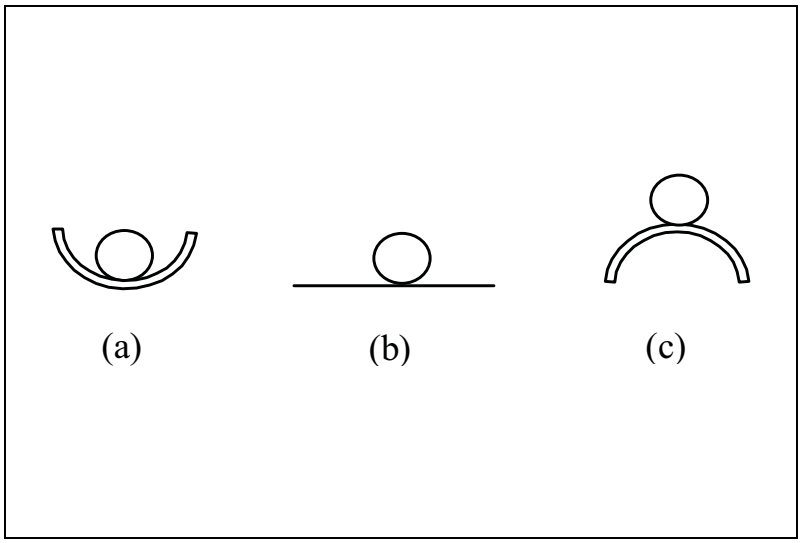

Figure 5: Stability Concept

Let us now consider an axially loaded cylinder not immersed in fluid. Take as an example a standing cylinder weighting ***x*** lbs. If a pull force of ***¾ x*** lbs. is applied at the top of the cylinder, then the support at the bottom will react with a force ***¼ x*** lbs. as shown in figure 6. There is, therefore, negative axial stress (compression) for a ***¼*** of the height, ***H***, of the cylinder from the bottom end. The point at depth ***¾ H*** will have zero axial stress. If we were to cut the cylinder at this plane, then the tension in the wire will not be affected. This implies that the point at depth *¾ H* is the neutral zone.

By submerging the cylinder in a fluid of density, ρ, and maintaining a perfect seal on the bottom of the cylinder, the point of zero axial stress remains at depth ***¾ H***.

But if we want to cut the cylinder at a point where the tension in the wire remains unchanged, then this point would be at depth, ***z***;

$$z = \frac{\frac{3}{4}x}{\frac{x}{H} - \rho g A}$$

... 15

where, ***A***, is the cross sectional area of the cylinder, ***g***, is the acceleration due to gravity, and ***x/H*** is the weight per unit length.

Therefore, the buoyancy affected the neutral point. Note that in both cases, at the neutral point and before cutting the cylinder the stresses were equal. In the case where the cylinder was not immersed in a fluid the stresses were;

$$\sigma_a = \sigma_r = \sigma_h = 0$$

... 16

In the case where the cylinder is immersed in a fluid the stresses were[#];

$$\sigma_r = \sigma_h = -P = -\rho g z$$

... 17

$$\sigma_a = -\frac{\frac{x}{H}(z - \frac{3}{4}H)}{A} \text{ or simplifying gives } \sigma_a = -\rho g z$$

... 18

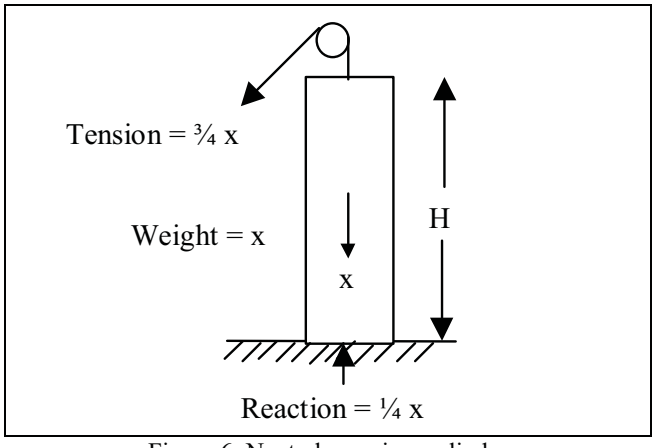

Figure 6: Neutral zone in a cylinder

[#] by substituting $P = P_o = P_i$ in eqns. 12 and 13

This leads to the conclusion that the point of neutral stability is located at the point where the isotropic stresses are equal. The cylinder is unstable in the region below the neutral stability and stable above. When the coiled tubing is stable, no buckling can occur.

2.9 Buckling

In an inclined well, the coiled tubing gets additional support from the walls. Paslay and Bogy[3] carried out a lengthy mathematical derivation of the critical compressive force, $F_{c\text{-}sin}$, necessary to initiate buckling in an inclined hole. Their analysis was further simplified by Dawson and Paslay[4] who derived the expression;

$$F_{c-\sin} = 2\sqrt{\frac{EIW\sin\bar{\theta}}{r}}$$

... 19

where E is the material Young modulus of elasticity, I is moment of inertia $I = \frac{\pi}{64}\left(d_o^4 - d_i^4\right)$ and r is the radial clearance between the coiled tubing and the hole. At the first instance the buckling will assume a sinusoidal form. However, if the lateral displacements are constrained (i.e. a wall constraint), then contact of the buckled coiled tubing with the constraint will induce a rearrangement to a helix form. Chen, Lin, and Cheatham[5] derived the critical force at which helical buckling is initiated, $F_{c\text{-}hel}$;

$$F_{c-hel} = \sqrt{2}F_{c-\sin}$$

... 20

A buckled coiled tubing will exert a further contact force with the constraint. In helical buckling mode, Mitchell[6] derived an expression for this force per unit length as;

$$F_{N-hel} = \frac{rT^2}{4EI}$$

... 21

There is no known reference for the contact force when in sinusoidal buckling. However, it is interesting to note that the normal contact force at the initiation of helical buckling is twice that of a non-buckled tube ($\Delta\theta$ and $\Delta\phi$ are set to zero in equation 5 while $F_{c\text{-}hel}$ is substituted for T in equation 21). A sensible assumption, but

not at all proven mathematically, would be to use a function, such as a linear one, ranging between the two contact forces[#].

2.10 Bending Stress

When the coiled tubing is in buckling or is travelling through a dogleg, a bending stress exists. This stress is due to the bending moment, which causes elongation of the coiled tubing on outer curve and shortening on the nearer curve. In the case of a buckled pipe, the bending stress, σ_b, acts in the axial direction and was derived by Lubinski et al[7];

$$\sigma_b = \frac{rTd_o}{4I}$$

... 22

Therefore, when the coiled tubing is in a buckling mode, the bending stress must be included in the axial stress term, i.e. equation (11) becomes;

$$\sigma_a = \frac{T}{\frac{\pi}{4}\left(d_o^2 - d_i^2\right)} + \frac{rTd_o}{4I}$$

... 23

The bending stress caused by doglegs is:

$$\sigma_b = \frac{d_o E}{2R + d_o}$$

… 24

where R is the Radius of curvature.

2.11 Lockup

Coiled tubing lockup is a term used to refer to a particular condition in which no coiled tubing movement or forces can be transmitted downhole. Normally, lockup is said to occur when the weight of the coiled tubing, as seen at surface, drops dramatically over a very short slack off distance.

Physically, the coiled tubing would go through a sequence of sinusoidal buckling and helical buckling. The bottom section of the coiled tubing will not suffer any buckling, but further up the well, parts of the coiled tubing will be in sinusoidal buckling followed by parts in helical buckling. The helically buckled coiled tubing

[#] The suggestion of this assumption was made during private communiqué with Suri Suryanarayana of Mobil Exploration and Producing Technical Center at Dallas, Texas.

could extend all the way to surface. In the parts of the coiled tubing that are helically buckled, the normal contact force, given by equation 21, increases rapidly eventually reaching an asymptote. This contact force will cause the friction force to increase proportionally thus reducing the weight seen at surface.

The maximum reach of a helically buckled coiled tubing in a horizontal well can be determined as follows;
Notes:

1. Equation (5) is used with $\bar{\theta} = 90^o$ and $\Delta\theta = \Delta\phi = 0$ to produce equation (25)
2. The analysis is only concerned with helically buckled portion of coiled tubing.
3. The compression, ***T***, is considered positive.

- the normal force between coiled tubing and the well bore is given by;

$$F_N = W$$

... 25

- the total normal force when in helical buckling is;

$$F_{N-total} = W + \frac{rT^2}{4EI}$$

... 26

- the increment in the compressive force is given by;

$$\Delta T = \mu \Delta x (W + \frac{rT^2}{4EI})$$

... 27

where ***Δx*** is the segment length. This equation can be rewritten as;

$$\frac{dx}{dT} = \frac{1}{\mu}\sqrt{\frac{4EI}{rW}}\left\{\frac{\sqrt{\frac{4EIW}{r}}}{\frac{4EIW}{r} + T^2}\right\}$$

... 28

aside;

$$\int \frac{a}{a^2 + x^2} dx = \tan^{-1}\frac{x}{a} + const$$

- integrating gives;

$$x = \frac{1}{\mu}\sqrt{\frac{4EI}{rW}}\tan^{-1}\left\{\frac{T}{\sqrt{\frac{4EIW}{r}}}\right\} + C$$

- imposing the boundary condition at $\boldsymbol{x = 0,\ T = T_o}$, i.e. $\boldsymbol{T_o}$ is the tension/compression at the bottom of the helically buckled coiled tubing.

$$C = -\frac{1}{\mu}\sqrt{\frac{4EI}{rW}}\tan^{-1}\left\{\frac{T_o}{\sqrt{\frac{4EIW}{r}}}\right\}$$

... 29

- substituting and rearranging gives;

$$T(x) = 2\sqrt{\frac{EIW}{r}}\tan\{\mu x\sqrt{\frac{rW}{4EI}} + \tan^{-1}[T_o\sqrt{\frac{r}{4EIW}}]\}$$

... 30

- Jian Wu and H.C.Juvkam-Wold[8] deduced that lockup would occur when

$$\mu x\sqrt{\frac{rW}{4EI}} + \tan^{-1}[T_o\sqrt{\frac{r}{4EIW}}] = \frac{\pi}{2}$$

... 31

- the expression in (31) could be simplified to yield the maximum helically buckled length in a horizontal well;

$$x_{\max} = \frac{0.6155\sqrt{\frac{4EI}{rW}}}{\mu}$$

... 32

In practice the coiled tubing will be subjected to a combined axial and bending stress greater than the minimum yield stress, $\boldsymbol{\sigma_y}$, well before satisfying the condition depicted by (31). Indeed, the distance $\boldsymbol{x_{max}}$ can only be approached but never attained as the compressive force ***T(x)*** would have to be infinite before satisfying this

condition. Figure 7 shows the growth of the compressive force for helically buckled coiled tubing in a horizontal well without any compressive force at the bottom (equation 30 with $T_o = 0$).

Furthermore, when performing computer simulations the numbers will be too large for the computer to handle. Therefore, there is a need to mathematically define a lockup criterion that will be physically possible and can be calculated by the computer. Substituting the combined axial and bending stress and the minimum yield stress in equation (14) and rearranging gives the critical compressive force at which the coiled tubing will yield, T_{yld};

$$T_{yld} = \frac{\sigma_r + \sigma_h - \sqrt{4\sigma_y^2 + 6\sigma_r\sigma_h - 3\sigma_r^2 - 3\sigma_h^2}}{2\left(\frac{rd_o}{4I} + \frac{1}{A}\right)} \quad \text{... 33}$$

where A is the cross sectional area of the coiled tubing. Equation (33) represents the limit at which permanent corkscrewing would occur. Lubinski *et al*[7] gave two expressions for the stresses on the inner and outer walls, at which permanent corkscrewing would occur, by substituting the radial and hoop stresses expressions in (33).

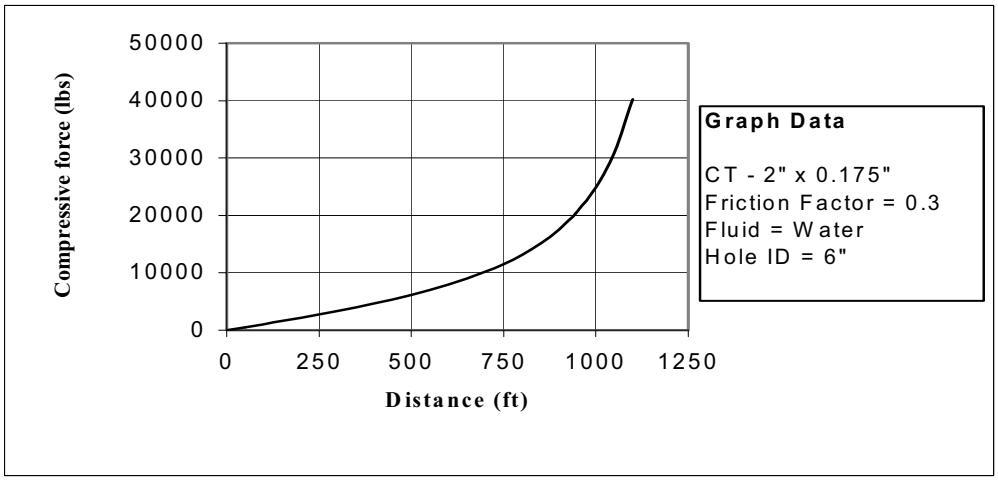

Figure 7: Compressive force at the top of a helically buckled coiled tubing in a horizontal well

2.12 Weight on Bit (WOB)

When drilling with coiled tubing, there is normally a need to apply a WOB to assist in drilling. Any WOB will imply a change in the boundary condition stated in equation (1). The modified end force will have to include the WOB;

$$F_{end} = W_{bha}\cos\theta - P_o\frac{\pi}{4}d_o^2 + P_i\frac{\pi}{4}d_i^2 \pm Friction_{bha} - WOB$$

... 34

Applying equation (34) and then working through the procedure of computing the tension/compression, as detailed in the previous sections, will enable us to predict the weight readings while applying a given WOB. Also, working in the opposite way is possible because we have a boundary condition. That is, if we have a weight reading at surface while drilling, we can directly predict the WOB provided no lockup occurs.

2.13 Maximum Weight on Bit

The effect of the WOB is to induce buckling in the coiled tubing at an earlier depth. As we have seen earlier, coiled tubing lockup can occur under such circumstances. When lockup does occur, any push force exerted from surface will almost all be dissipated to overcome the friction due to the increased normal contact force. If, however, the yield limit is reached before lockup occurs, then we risk plastically deforming the coiled tubing. Therefore, we can only apply a maximum WOB, which corresponds to the lockup occurring, as defined by equation (33).

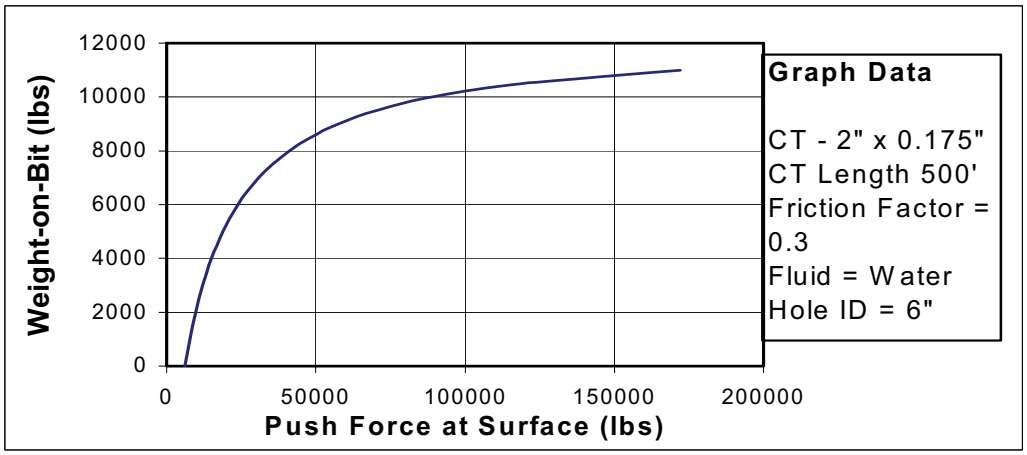

Figure 8: Force-in versus force-out in a horizontal well

Figure 8 shows the effect of increasing the initial compressive force, $\boldsymbol{T_o}$ in equation (30), on the compression at the top of a fixed length coiled tubing in a horizontal well. The curve can be interpreted as the relationship between the compressive force required at the top of 500-ft coiled tubing to produce the WOB at the lower end. Note that the curve is continuously changing slope towards horizontal, and the compressive force is becoming too large for the coiled tubing to tolerate without plastically deforming or even collapsing.

The procedure to compute the maximum WOB is a trial and error one. An initial WOB at which lockup occurs is estimated then the procedure for computing the tension/compression is carried out. If lockup occurs anywhere in the well during this

computation then the initial guess has to be reduced, if lockup does not occur then the initial guess has to be increased. This iterative procedure has to be repeated until a convergence criterion of the maximum WOB, without lockup occurring, is reached. Note that it will not be possible to use a convergence criterion of the weight at surface, as this will change dramatically when approaching lockup.

2.14 Maximum Over Pull

The maximum over-pull is determined by substituting the minimum yield stress, σ_y, of the coiled tubing in the Von Mises relationship, then solving for the axial stress, σ_a.

$$\sigma_a = \frac{(\sigma_r + \sigma_h) \pm \sqrt{4\sigma_y^2 + 6\sigma_r\sigma_h - 3\sigma_r^2 - 3\sigma_h^2}}{2}$$

... 35

The axial stress is then multiplied by the cross-sectional area of the coiled tubing, A, to yield the maximum over-pull available. Note that only the positive sign of the square root needs to be considered as the negative sign will give a compressive axial stress (hint: set the radial and hoop stresses to zero).

2.15 Nomenclature

A_i	Internal coiled tubing area
C_D	Coefficient of fluid drag force
D	Fluid drag force
d_c	Capillaries diameter
d_i	Coiled tubing inner diameter
d_o	Coiled tubing outer diameter
E	Young modulus of elasticity
$F_{c\text{-}sin}$	Critical compressive force at which coiled tubing will sinusoidally buckle
$F_{c\text{-}hel}$	Critical compressive force at which coiled tubing will helically buckle
F_{end}	End force at the bottom of the coiled tubing
F_N	Normal contact force
$Friction_{bha}$	Friction on bottom hole assembly
g	Acceleration due to gravity
I	Inertia of coiled tubing
P_i	Internal coiled tubing pressure
P_o	Pressure outside the coiled tubing, or pressure in the well
R	Radius of curvature
Re	Reynolds number, representative of inertia to viscous forces
r	Radial clearance between coiled tubing and wellbore
r_d	Radial distance
r_i	Internal radius of coiled tubing
r_o	Outer radius of coiled tubing

S	Coiled tubing segment outer surface area
T	Tension/compression (tension is positive)
T_{yld}	Tension/compression at which the coiled tubing material will yield
V	Fluid relative velocity passed coiled tubing
V_{bha}	Volume of bottom hole assembly
W	Buoyed weight of coiled tubing
WOB	Weight on bit
W_{bha}	Buoyed weight of the bottom hole assembly
W_c	Capillaries weight per unit length
Wt_{bha}	Weight of bottom hole assembly
x	Distance
z	Height
ϕ	Well azimuth
η	Fluid viscosity
μ	Force friction factor
θ	Well deviation
$\bar{\theta}$	Segment of well average deviation
ρ_i	Density of fluid inside coiled tubing
ρ_o	Density if fluid in the well, outside the coiled tubing
σ	Tri-axial stress
σ_a	Axial stress component
σ_b	Bending stress
σ_h	Hoop or circumferential stress component
σ_r	Radial stress component
σ_y	Coiled tubing minimum yield stress

2.16 References

1. Johancsik, C.A., Friesen, D.B., and Dawson, Rapier "Torque and Drag in Directional Wells - Prediction and Measurement", JPT, June 1984, pp.987-992.
2. Love, A.E.H. "A Treatise on the Mathematical Theory of Elasticity", 4th ed., Dover Publications, New York City (1944) 144.
3. Paslay, P.R. and Bogy, D.B. "The Stability of a Circular Cylinder Rod Laterally Constrained to be in Contact with an Inclined Circular Cylinder", J.Appl.Mech. (1964), 31, pp.605-610.
4. Dawson, Rapier and Paslay, P.R. "Drillpipe Buckling in Inclined Holes", JPT, Oct.1984, pp.1734-1738.
5. Chen, Y.C., Lin, Y.H., and Cheatham, J.B. "An Analysis of Tubing and Casing Buckling in Horizontal Wells", OTC 6037, Houston, May 1989, pp.617-620.
6. Mitchell, R.F. "Simple Frictional Analysis of Helical Buckling of Tubing", SPE Drilling Engineering 13064, Dec.1986, pp.457-465.
7. Lubinski, Arthur, Althouse, W.S., and Logan, J.L. "Helical Buckling of Tubing Sealed in Packers", JPT, June 1962, pp.655-670.
8. Wu, J. and Juvkam-Wold, H.C. "Drilling and Completing Horizontal Wells with Coiled Tubing", 68th Annual Technical Conference and Exhibition, SPE, Houston, Oct. 1993.

3. FATIGUE ANALYSIS

The stress-strain relationship given by Hook's law, dictates that the coiled tubing must not exceed the minimum yield stress, σ_y, to remain within the elastic range of the curve. Since the slope of the curve is given by the Young modulus, E, the following condition for the strain, ε, must be satisfied;

$$\varepsilon \leq \frac{\sigma_y}{E} \qquad \text{... 36}$$

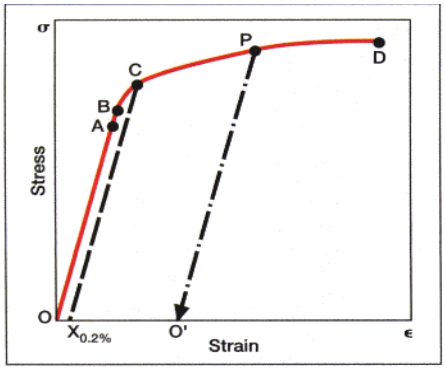

Figure 9: Hook's law for the stress-strain relationship

If we were to substitute the values of the minimum yield stress and the Young modulus of elasticity for coiled tubing QT-700, say, then we obtain a maximum strain of $7/3 \times 10^{-3}$ ($E = 30 \times 10^6$ psi, $\sigma_y = 70{,}000$ psi).

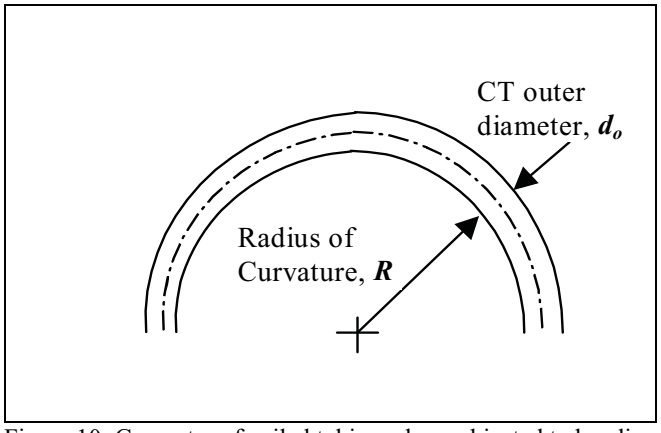

Figure 10: Geometry of coiled tubing when subjected to bending

3.1 Effect of Equipment Size

In figure 10, if we assume the radius of curvature over which the coiled tubing is being bent to be ***R***, and the coiled tubing outer diameter to be d_o then the length of the non-deformed coiled tubing is given by;

$$L = 2\pi(R + \frac{d_o}{2})$$

... 37

while the length of the outer side of the coiled tubing is given by;

$$L + \Delta L = 2\pi(R + d_o)$$

... 38

therefore, the strain can be calculated as;

$$\varepsilon = \frac{\Delta L}{L} = \frac{d_o}{2R + d_o}$$

... 39

or

$$R = \frac{d_o}{2}(\frac{1}{\varepsilon} - 1)$$

... 40

Thus, if we were to keep a 2" QT-800 coiled tubing (typical for coiled tubing used in drilling applications) within the elastic range at all times, the radius of curvature must be greater than 31.2 ft. This implies that the gooseneck must have a radius of 32 ft and the reel must have a core diameter of 63 ft. Clearly such dimensions are not acceptable because of the costs involved in building such equipment and the difficulties of transporting them. As a result, the coiled tubing equipment are built with reasonable sizes which unfortunately dictates that the coiled tubing will suffer plastic deformation.

3.2 Effects of Axial Stress on Fatigue Life

As a result, the coiled tubing is subjected to stresses higher than the minimum yield stress when travelling from the reel to the gooseneck and from the gooseneck into the injector, as shown in figure 11. During this journey, the coiled tubing is

subjected to 3 plastic deformation cycles and on the journey out of the well a further 3 plastic deformation cycles are experienced[1].

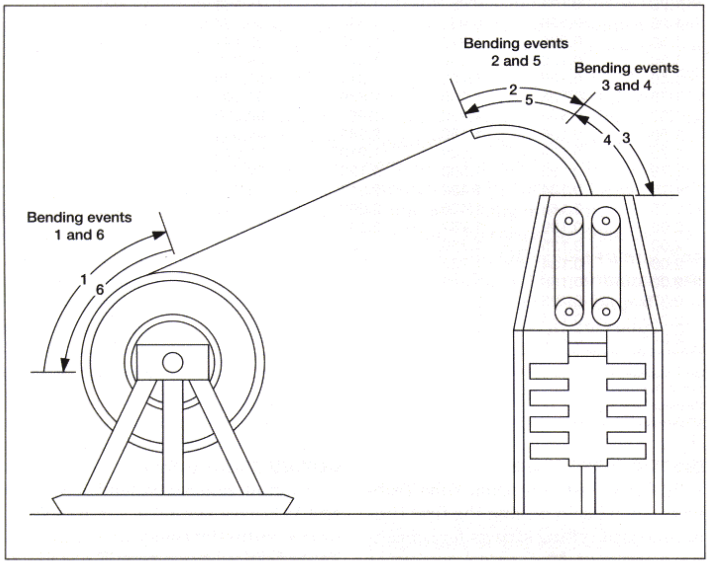

Figure 11: Plastic deformation cycles of coiled tubing during running in and pulling out of a well

Figure 12, shows the effects of stresses on the number of cycles that could be attained before fatigue failure ensues[2]. The figure shows two curves intersecting at the point corresponding to the normalised minimum yield stress (on the Y-axis). To use this figure, the normalised stress should be determined first then go across horizontally until intersecting with the upper of the two curves.

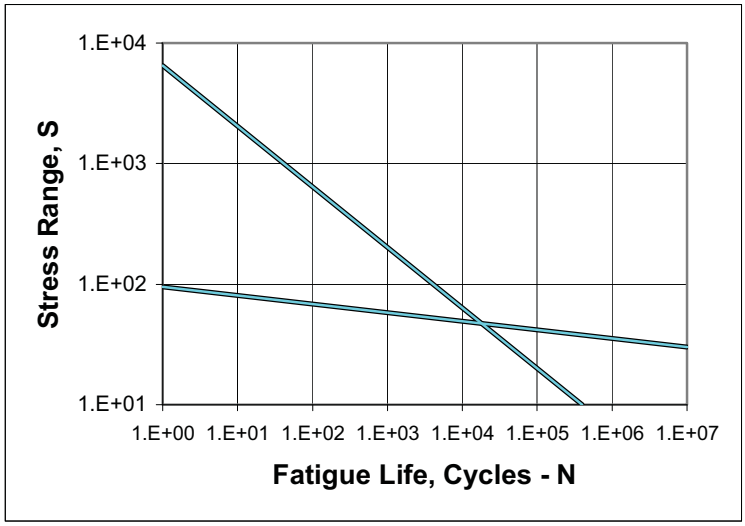

Figure 12: Low-cycle S-N Line (Avakov et al, 1993)

As can be seen, within the elastic range the number of cycles would be in the order of 10^4 and more while in the plastic range the number of cycles is reduced significantly.

An equation of the form $S = aN^{\alpha} + bN^{\beta}$ will sufficiently describe the upper bound curve of figure 12. The term aN^{α} represents the elastic range while the term bN^{β} represents the plastic range. Since the coiled tubing is being used in the plastic range, the first term of the equation can be neglected. Hence, we can rewrite the equation as;

$$S = bN^{\beta}$$

... 41

The power index β has a value of -½. Using empirical median life in cycles, N_m, and median fatigue strength, S_m, found by tests, we can write an expression for the fatigue damage, λ, caused by a stress cycle as;

$$\lambda = \frac{(S / S_m)^2}{N_m} \times 100\%$$

... 42

The value given in the literature for S_m is 1000 and for N_m is 130. As we have seen before, the coiled tubing goes through 2 cycles of plastic deformation on the reel and further 4 on the gooseneck. Each of these cycles induces axial stress, which can be calculated as follows;

- Over the gooseneck the axial stress, S_{ag}, is;

$$S_{ag} = \frac{d_o E}{2R_g}$$

... 43

where R_g is the gooseneck radius.

- Over the reel the axial stress, S_{ar}, is;

$$S_{ar} = \frac{d_o E}{D_R}$$

... 44

where D_R is the reel diameter.

3.3 Effects of Pressure

Internal coiled tubing pressure induces further hoop (circumferential) and radial stresses. The additional stresses due to the internal pressure will adversely affect the coiled tubing life because they will increase the overall stress, i.e. moving

upwards on the Y-axis of figure 12. Note, however, if no axial stress were present (no movement of coiled tubing taking place simultaneously), then the stresses due to the internal pressure will only be within the elastic range thus having an insignificant effect on the coiled tubing life.

The additional stress component due to the internal pressure can be computed as;

$$S_t = \frac{2d_i^2 P_i}{d_o^2 - d_i^2}$$

... 45

The total stress is computed using an empirical formula and is given as;

$$S = S_a + S_t^{1.895}$$

... 46

Equation (45) is applicable to both cases of the stress over the gooseneck and the reel, where S_a is the axial stress.

3.4 Effects of Weight

The coiled tubing parts being held by the chain blocks support the weight of the coiled tubing in the well. This part of the coiled tubing is not being subjected to any bending, thus the stresses are only due to the weight of the coiled tubing and any additional stresses due to pressure. However, since in practice these stresses are always kept below the minimum yield stress, the cycling in this section will not affect the coiled tubing life significantly.

3.5 Other Effects

- **Material Strength**

  Higher strength coiled tubing will be able to sustain more fatigue cycles. This effect is included in a strength factor, F_m, which is a function of the reduction in area, RA, in fractions

$$F_m = \{\frac{\ln(1 - RA)}{\ln(0.47)}\}^2$$

... 47

The factor RA has a value of 0.53 for QT-700 and 0.57 for QT-800 or equivalent.

- **Welds**

  The effect of welds is to induce stress concentration locally. Depending on the type of weld used, a weld factor, F_w, will reflect the effect. Typical values for weld factor are 0.7 for smoothly dressed butt-welded section, 0.5 for poorly dressed butt-welded section, and 0.31 for undressed butt-welded section.

- **Corrosion**

  Acid corrosion is rare in coiled tubing drilling applications. However, when H_2S sour gas is encountered then corrosion will be important. The two corrosion effects are different in nature. The acid will corrode the material of the coiled tubing and reduces the wall thickness while the sour gas molecules will embed themselves in between the material molecules thus inducing stress concentration.

  A corrosion factor, F_c, is normally used to account for either effect. Typical values for the corrosion factor are 0.66 for 15% HCl acid and 0.5 for H_2S gas.

- **Reliability of Empirical Data**

  A reliability factor, F_R, is also introduced to reflect the confidence in the test data. The reliability factor is a function of the reliability level, Q, and is given as;

$$F_R = 11.47^{\left(\frac{\ln Q^{\frac{1}{15}}}{\ln 0.5} - 1\right)}$$

... 48

Equation (42) is modified to include all the above factors;

$$\lambda = \frac{1}{F_m F_w F_c F_R} \times \frac{\left(S / S_m\right)^2}{N_m} \times 100\%$$

... 49

3.6 Nomenclature

D_R	Reel diameter
d_i	Coiled tubing inner diameter
d_o	Coiled tubing outer diameter
E	Coiled tubing Young Modulus of elasticity
F_c	Corrosion factor
F_m	Material strength factor
F_R	Reliability factor
F_w	Weld factor

L	Length
N	Number of cycles
N_m	Median number of cycles
P_i	Internal pressure in coiled tubing
Q	Reliability level
R	Radius of curvature
R_g	Gooseneck radius of curvature
RA	Reduction in area
S	Normalised stress
S_{ag}	Axial stress on gooseneck
S_{ar}	Axial stress on reel
S_m	Median normalised stress
S_t	Hoop or circumferential stress
ε	Coiled tubing strain due to elongation
λ	Fatigue damage
σ_y	Coiled tubing minimum yield stress

3.7 References

1. Sas-Jaworsky II, Alexander "Coiled Tubing … Operations and Services, Part 3 - Tube Technology and Capabilities", World Oil, Feb. 1992.
2. Avakov, V.A., Foster, J.C., and Smith, E.J. "Coiled Tubing Life Prediction" OTC 7325, 25th Annual OTC, Houston, May 1993.

4. FLUID CIRCULATION

In any drilling operation, fluid circulation is necessary for several reasons. In coiled tubing drilling the reasons include the cuttings transport, maintaining a given pressure opposite the reservoir, and lubrication. For these reasons, when a fluid circulation analysis is carried out the most important computed parameters include the fluid velocity and pressure.

There are essentially two types of flow that may be considered, single-phase and multi-phase flow.

4.1 Single Phase Flow

Only one fluid phase exists in the well and/or the coiled tubing. This phase will normally be liquid. It is rare to have gas only in the well because most gas wells will produce condensate and drilling using only gas is not common.

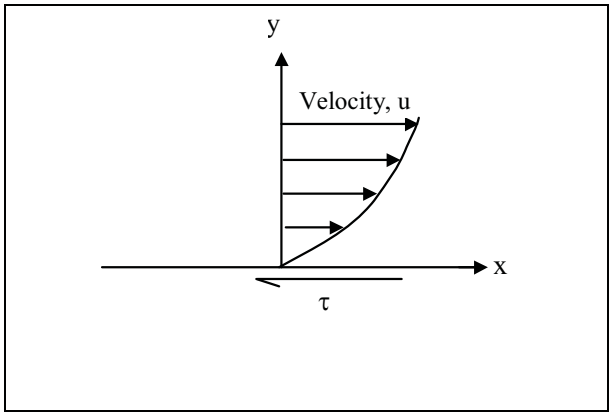

Figure 13: Newton's Definition of Viscosity

The fluid's viscosity can be either a constant, thus conforming to Newton's definition of viscosity, or can vary depending on the fluid shear rate. The first type of fluid is referred to as a Newtonian fluid while the Non-Newtonian fluids are also referred to as Generalised Newtonian fluids. Newton's definition of the viscosity is that it is the constant of proportionality between the shear stress, τ, and the shear rate, γ, in the direction perpendicular to the flow. In unidirectional flow this definition can be written as;

$$\tau = \eta \frac{\partial u}{\partial y} \qquad \textbf{... 50}$$

and in general,

$$\tau = \eta\gamma$$

... 51

Non-Newtonian fluids have a viscosity that behaves as a function of the shear rate. Several mathematical models to describe the shear stress – shear rate relationship exist. The most popular of these models, in the oil and gas industry, are the Power Law and the Bingham Plastic models.

The Power Law model can be used to describe shear thinning or shear thickening behaviour. Typically, most drilling fluids are shear thinning which means that when the fluid is being pumped it's viscosity is reduced thus reducing the required pumping pressure, but when little or no pumping is taking place then the fluid viscosity increases thus increasing the cuttings suspension. Paint is a typical example of shear thickening fluids where the viscosity is increased by shearing the paint. The Power Law model uses a Power Index, ***n***, (hence the name) to account for the above behaviour. When ***n*** has a value of unity the model reduces to a Newtonian fluid. For shear thinning fluids ***n*** takes a value smaller than unity and for shear thickening greater than unity. The shear stress is given by;

$$\tau = K\gamma^n$$

... 52

The parameter, ***K***, is referred to as the consistency factor, the reason being in equation (52) the units become inconsistent when ***n*** is other than unity, thus ***K*** will take the necessary units to achieve the consistency.

The Bingham Plastic model describes a fluid behaviour similar to solids, i.e. according to Hooke's law. That is, the fluid will not move until the yield stress, ***YP*** (known as the Yield Point), has been exceeded and when in motion the viscosity holds a constant value, ***PV*** (known as the Plastic Viscosity), and is in the plastic range. The shear stress is given by;

$$\tau = YP + PV\gamma$$

... 53

Other mathematical models exist but are seldom used in the oil and gas industry. The Herschel Bulkly model is probably the most adaptable as it is a combination of both the Power Law and Bingham Plastic models. The shear stress in this model is given by;

$$\tau = YP + K\gamma^n$$

... 54

Note that in equation (54), when ***n*** is unity we obtain the Bingham Plastic model, when ***YP*** is zero we obtain the Power Law model, and when ***YP*** is zero and ***n*** is unity we obtain the Newtonian model.

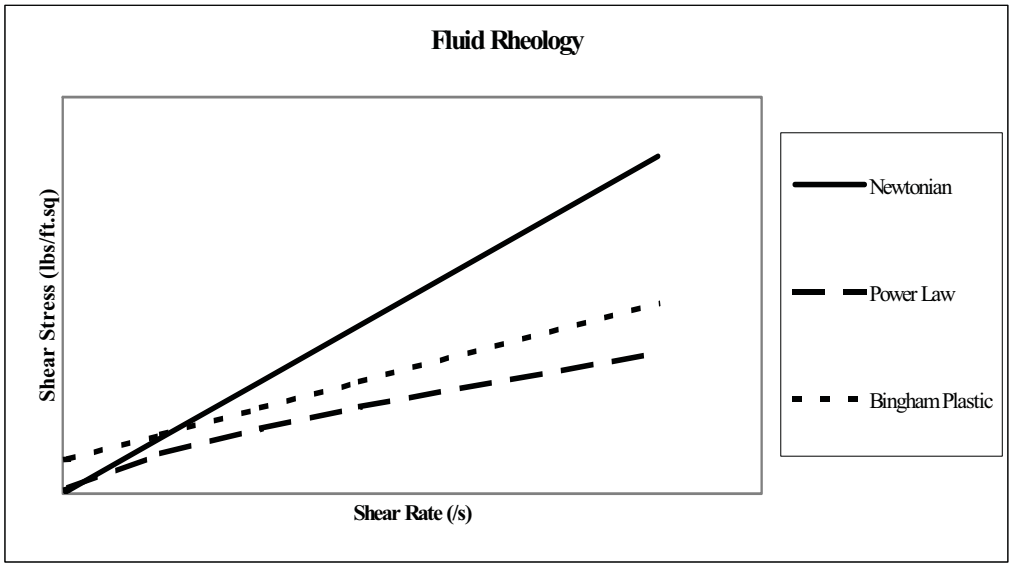

Figure 14: Shear stress – shear rate relationship for the various mathematical models used in the oil and gas industry.

4.2 Fluid Circulation Computations

The computations will start by computing the fluid velocity. In single-phase flow the fluid may be considered incompressible, thus the fluid velocity is constant as long as there are no changes in the borehole or coiled tubing geometry. The fluid velocity in pipe geometry is given by;

$$V = \frac{Q}{\frac{\pi}{4} d^2}$$

... 55

where ***Q*** is the flow rate and ***d*** is pipe internal diameter. Equation (55) applies equally inside the coiled tubing and in the parts of the well where no coiled tubing or other tubulars are inserted. In annular geometry, such as that between the borehole and the coiled tubing, the velocity is given as;

$$V = \frac{Q}{\frac{\pi}{4}(d_c^2 - d_o^2)}$$

... 56

where d_c is the borehole internal diameter and d_o is the coiled tubing outer diameter.

The pressure difference between two calculation nodes consists of two parts, the hydrostatic pressure difference ΔP_{hyd}, and the dynamic pressure difference ΔP_{dyn}. The hydrostatic pressure difference is given as;

$$\Delta P_{hyd} = \rho g \Delta tvd$$

... 57

where ρ is the fluid density, g is the acceleration due to gravity, and tvd is the true vertical depth of the node.

The dynamic pressure difference is given by[1];

$$\Delta P_{dyn} = 4f \frac{\rho V^2}{2} \frac{|\Delta Depth|}{d_w}$$

... 58

where f is the friction factor and is obtained from the Moody chart as a function of the Reynolds number and relative roughness. The parameter d_w is the equivalent diameter which in pipe geometry is equal to the pipe internal diameter, and in annular geometry is given as;

$$d_w = d_c - d_o$$

... 59

The Reynolds number is defined as the ratio of inertia to viscous forces and is given by;

$$\mathrm{Re} = \frac{\rho V d_w}{\eta}$$

... 60

where η is the fluid viscosity. The table in the appendix shows the various expressions to determine the pressure drop for the three rheological models in both pipe and annular flows.

4.3 Multi Phase Flow

In multi phase flow, two phases co-exist, liquid and gas. The gas is a compressible fluid, thus the volumetric flow rate will change depending on temperature and pressure conditions. Furthermore, when slip between the two phases exists, an acceleration term must be added to the pressure drop computations. Two types of multi phase flows are commonly used in coiled tubing drilling applications, foam and commingled gas and liquid[#]. In foam, a surfactant is added which prevents the slippage between the two phases.

4.3.1 Surface Tension

In multi phase flow, it is often necessary to obtain another fluid parameter known as the fluid surface tension. The fluid surface tension is a difficult parameter to obtain because not many fluid suppliers provide the necessary data. However, a simple measuring technique could be adapted to measure the fluid surface tension. If we were to place the fluid in a tank and immerse a capillary tube inside the tank, the fluid will rise due to the surface tension force. Thus, the fluid surface tension, σ, may be determined as follows;

- The surface tension force = $\sigma \pi d_{capillary}$
- The weight of the fluid column supported by the surface tension force = $\frac{\pi}{4} d_{capillary}^2 \rho g h$

where $d_{capillary}$ is the capillary diameter and h is the height to which the fluid rises. Therefore;

$$\sigma = \frac{d_{capillary} \rho g h}{4}$$

... 61

4.3.2 Compressibility of Gas

Nitrogen, N_2, is the most common gas used in coiled tubing drilling. Therefore, it is important that we should be able to determine the compressibility of Nitrogen. Fortunately, a curve fitting formula exists for computing the Nitrogen compressibility factor, z[3];

$$z = AP^2 + BP + C$$

... 62

[#] Commingled liquid and gas flow is also known as multi phase flow and for the remainder of this document the term multi phase flow will used to describe commingled flow.

A, B, and C are coefficients dependent on the temperature and the pressure range, while P is the absolute pressure in psia. The coefficients A, B, and C are given for different pressure ranges as;

- For $P \leq 500$; $A = 0$, $B = 0$, and $C = 1$
- For $500 < P \leq 4000$; $A = \alpha_o + \alpha_1 T + \alpha_2 T^2 + \alpha_3 T^3$, $B = \beta_o + \beta_1 T + \beta_2 T^2$ and $C = 1$
- For $4000 < P \leq 8000$; $A = 0$, $B = \beta_o + \beta_1 T + \beta_2 T^2$ and $C = \zeta_o + \zeta_1 T + \zeta_2 T^2$
- For $P > 8000$; $A = 0$, $B = \beta_o + \beta_1 T + \beta_2 T^2$ and $C = \zeta_o + \zeta_1 T + \zeta_2 T^2$

where T is the absolute temperature in ^oR (i.e. T = *temperature in* $^oF + 460$). The coefficients, α, β, and ζ are given in table 1.

	$500 < P \leq 4000$	$4000 < P \leq 8000$	$P > 8000$
α_o	1.679393e-07		
α_1	-6.2243e-10		
α_2	8.0385e-13		
α_3	-3.5472e-16		
β_o	-3.122e-04	2.2817e-04	2.2042e-04
β_1	8.488e-07	-4.066e-07	-3.515e-07
β_2	-5.37e-10	2.3e-10	1.815e-10
ζ_o		-0.0956	-0.1573
ζ_1		2.5e-03	2.438e-03
ζ_2		-1.5e-06	-1.4e-06

Table 1: Coefficients for determining the z-factor

For natural gas, the compressibility factor may be obtained from charts. Several of these charts exist in the literature and an example is shown in figure 15 for the most commonly found natural gas (specific gravity 0.65)[#].

[#] For other specific gravities see "The Technology of Artificial Lift Methods", Vol. I, by Kermit E. Brown and H. Dale Beggs[5].

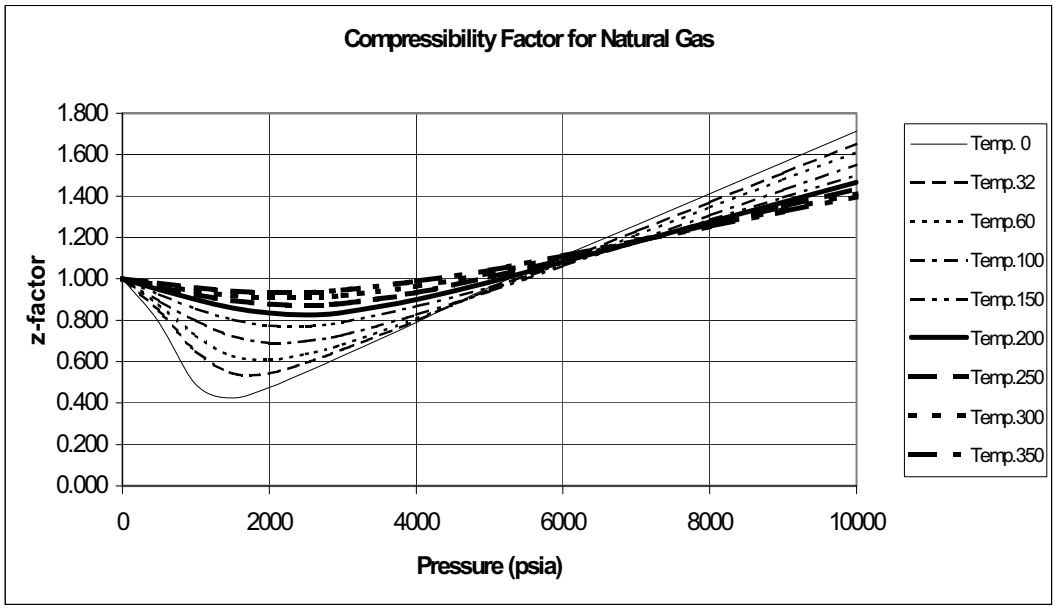

Figure 15: Compressibility factor for natural gas, specific gravity 0.65 (temperatures are in ^{o}F)

The gas volume factor, B_{gas}, is defined as the volume of gas at standard temperature and pressure that will occupy one unit volume of space at a given temperature and pressure. This factor can be derived from the theory of gases;

$$B_{gas} = \left(\frac{P}{P_s}\right)\left(\frac{T_s}{T}\right)\left(\frac{1}{z}\right)$$

... 63

In API English units, the standard temperature is $T_s = 60^oF = 520^oR$, and the standard pressure is $P_s = 14.65\ psia$. Thus the volume factor becomes;

$$B_{gas} = 199.3\left(\frac{P}{Tz}\right) \quad scf/bbl\ of\ space$$

4.4 Foam Flow

Blauer *et al*[4] conducted some tests to produce a general procedure for computing pressure losses for laminar, transitional, and turbulent foam flow. Their conclusions were that foam could be treated as a single-phase compressible fluid. The rheological properties of the foam being a function of the foam quality and the shear rate, as shown in figure 16.

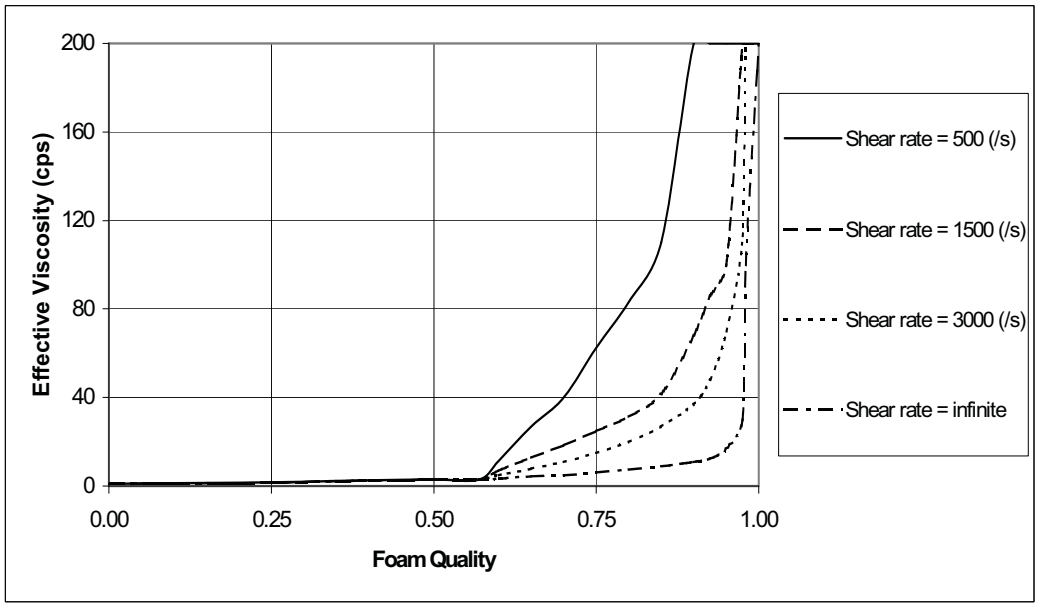

Figure 16: Effective Viscosity of Foam

4.5 Pressure Losses in Multi Phase Flow

Several methods have been documented to compute the pressure losses of multi phase flow[5]. The most popular methods adapted in the oil and gas industry include the Duns and Ros, Beggs and Brill, and the Hagedorn and Brown. All the methods compute a pressure gradient and require that pressures at two nodes be known beforehand. Normally, the pressure at the starting node is known, and the pressure at the next node is estimated. After computing the pressure gradient, the distance between the two pressures can be computed. If the distance does not match the depth difference between the two nodes, then a new estimate of the pressure at the next node is made and so forth until a convergence criterion is satisfied.

The Duns and Ros method is one of the best correlations that cover all ranges of flow. The range of their laboratory data is the most complete taken for this field of work. This method is based on computing a total non-dimensional pressure gradient, G, consisting of three components, the hydrostatic, G_{st}, the friction (or dynamic), G_{fr}, and the acceleration gradient, G_{ac}:

$$G = G_{st} + G_{fr} + G_{ac}$$

... 64

The dimensionless pressure gradient is expressed as a fraction of the hydrostatic liquid gradient $\rho_L g$, thus;

$$G = \left(\frac{1}{\rho_L g}\right)\left(\frac{dP}{dh}\right)$$

... 65

where dP/dh is the pressure gradient.

The flow is separated into three main regions and separate correlations for slippage and friction were developed for each region. Figure 17, shows the regions of the flow as suggested by Duns and Ros. When the flow is predominantly liquid it is said to be "bubble flow", and when predominantly gas it is said to be "mist flow". The region in the middle is referred to as "slug flow". Non-dimensional liquid and gas velocity numbers, N_{LV} and N_{gV}, based on the superficial liquid and gas velocities, V_{sL} and V_{sg}, are used to determine the boundaries between these regions. The "superficial velocities" are the equivalent velocities for each of the phases flowing alone.

The non-dimensional liquid velocity number is given as;

$$N_{LV} = V_{sL}\left(\frac{\rho_L}{g\sigma}\right)^{1/4}$$

... 66

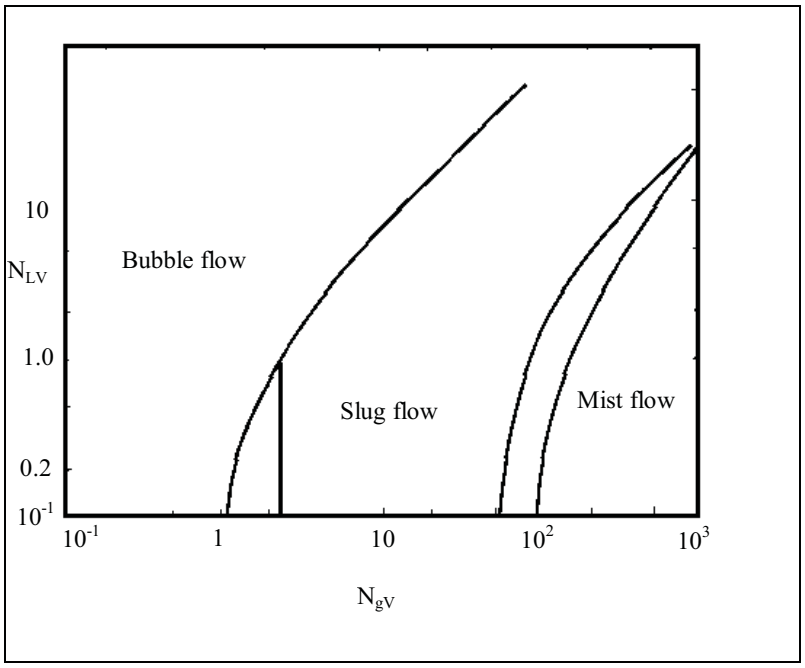

Figure 17: Multi phase flow regions

and the non-dimensional gas velocity number;

$$N_{gV} = V_{sg}\left(\frac{\rho_L}{g\sigma}\right)^{1/4}$$

... 67

Given that the average pressure and temperature are known, equation (63) is used to compute the volumetric flow rate of the gas phase. The superficial velocities are computed using each phase flow rate in either equation (55) or (56), depending on the geometry of the flow domain. The region boundaries are given as follows:

- Boundary between bubble and slug flows $N_{gV} \leq L_1 + L_2 N_{LV}$
- Boundary between slug flow and transition to mist flow
  $L_1 + L_2 N_{LV} < N_{gV} \leq 50 + 36\, N_{LV}$
- Boundary between transition to mist flow $N_{gV} > 75 + 84\,(N_{LV})^{0.75}$

The parameters L_1 and L_2 are determined from figure 18, where N_d is the diameter number and is given as;

$$N_d = d_w\left(\frac{\rho_L g}{\sigma}\right)^{1/2}$$

... 68

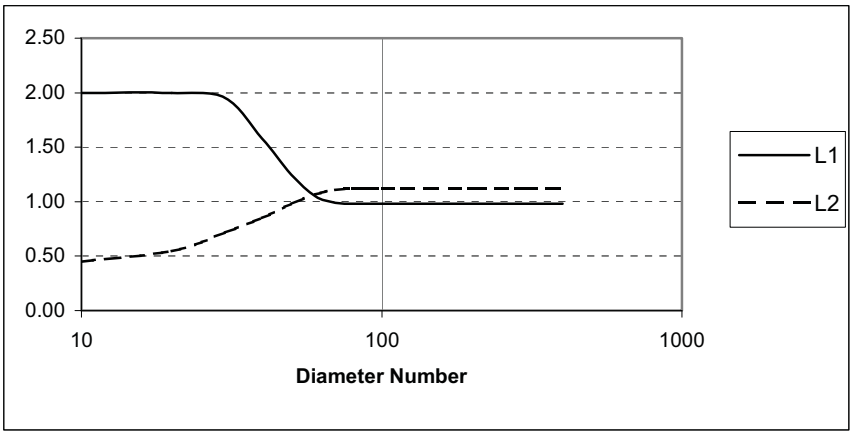

Figure 18: L-factors against N_d

For each region, a slip factor, ***S***, is introduced and is determined as follows;

- For bubble flow

$$S = F_1 + F_2 N_{LV} + \left(F_3 - \frac{F_4}{N_d} \right) \left(\frac{N_{gV}}{1 + N_{LV}} \right)^2$$

- For slug flow

$$S = \left(1 + F_5\right) \frac{N_{gV}^{0.982} + 0.029 N_d + F_6}{\left(1 + F_7 N_{LV}\right)^2}$$

- For mist flow

$$S = 0$$

The factors F_1 through to F_7 are determined from figures 19 through to 22, where N_L is the liquid viscosity number and is given by;

$$N_L = \eta \left(\frac{g}{\rho_L \sigma^3} \right)^{1/4}$$

... 69

The slip velocity, V_S, is then computed as;

$$V_S = \frac{S}{\left(\frac{\rho_L}{g\sigma} \right)^{1/4}}$$

... 70

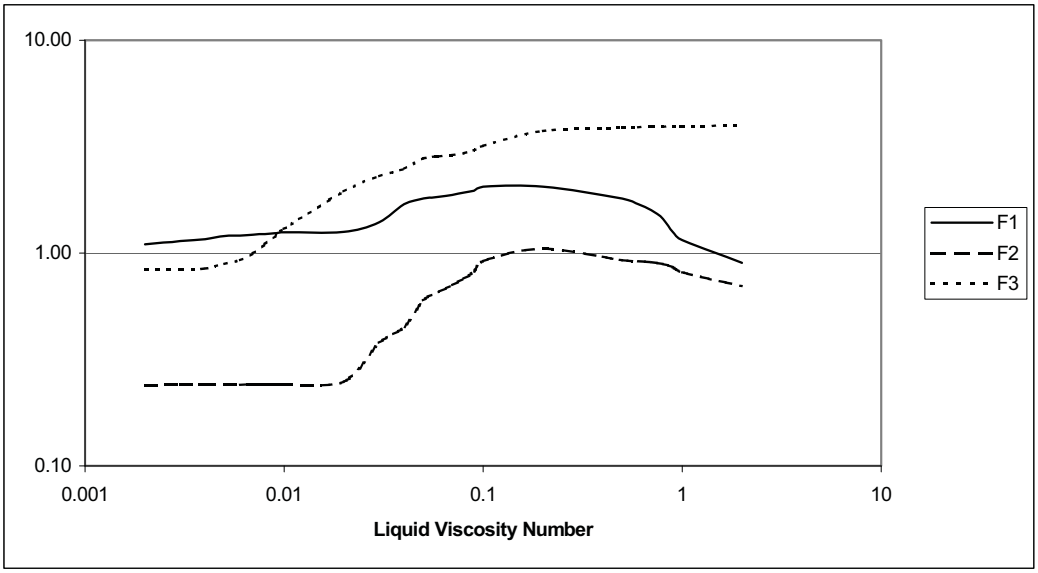

Figure 19: Factors F_1, F_2, and F_3

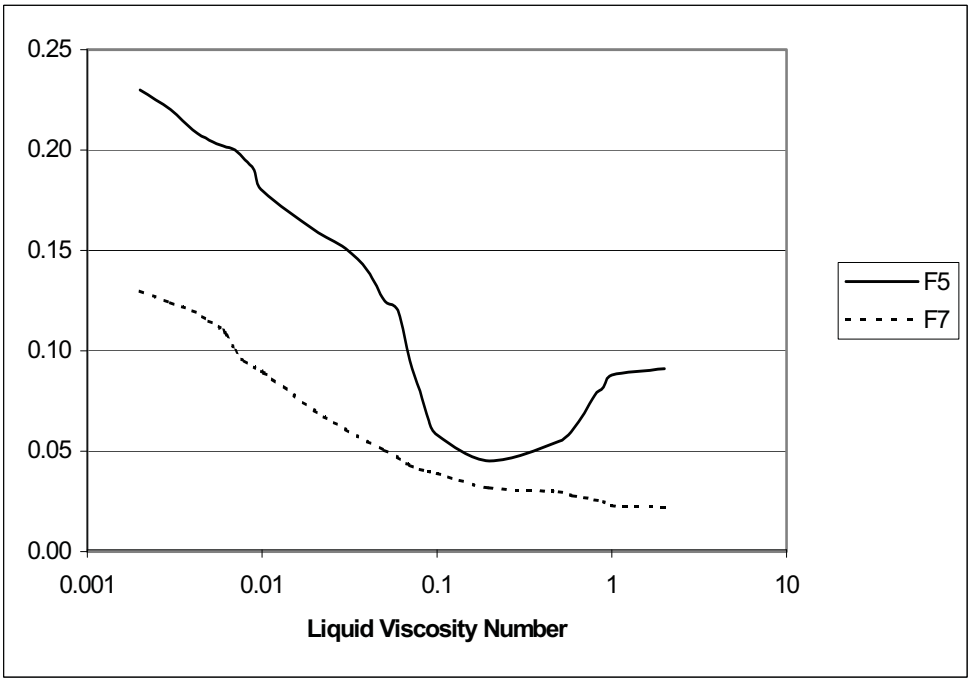

Figure 20: Factors F_5 and F_7

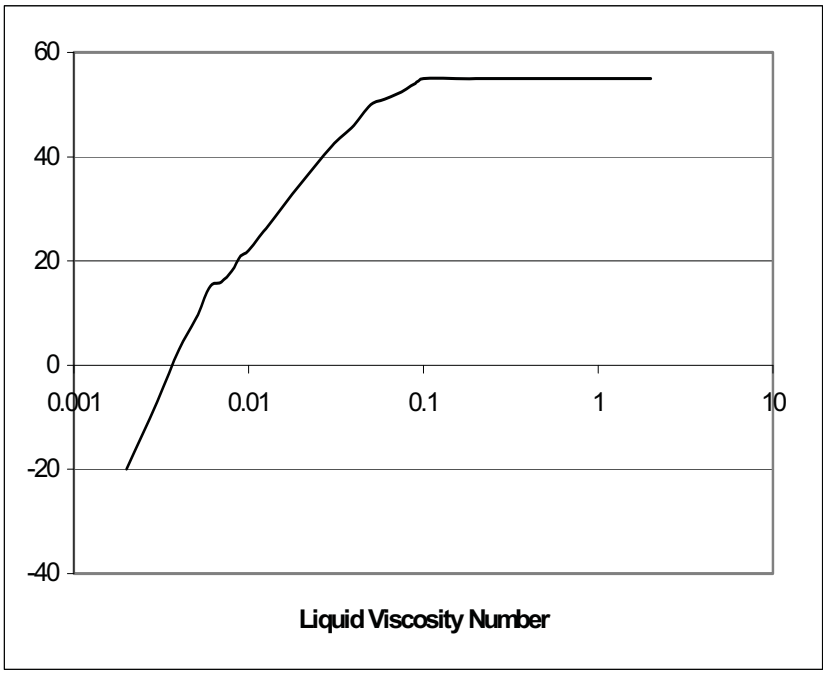

Figure 21: Factor F_4

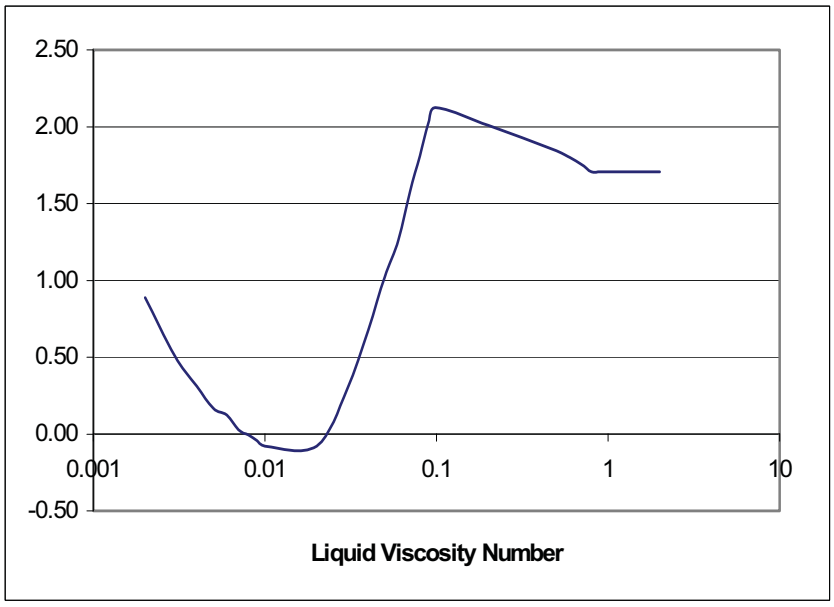

Figure 22: Factor F_6

It was found that the liquid hold-up, H_L, is related to the slip velocity as follows;

$$V_S = \frac{V_{sg}}{1-H_L} - \frac{V_{sL}}{H_L}$$

... 71

Equation (71) is rearranged to give the liquid hold-up in terms of the slip and superficial velocities;

$$H_L = \frac{V_S - V_{sg} - V_{sL} + \sqrt{\left(V_S - V_{sg} - V_{sL}\right)^2 + 4V_S V_{sL}}}{2V_S}$$

... 72

The hydrostatic pressure gradient can now be computed as follows;

$$G_{st} = H_L + \left(1-H_L\right)\frac{\rho_g}{\rho_L}$$

... 73

where the gas density, ρ_g, is computed using the gas volume factor, equation (63), and the gas specific gravity, γ_g, thus in API English units;

$$\rho_g = 0.0764\gamma_g B_{gas} \qquad (\text{lb}_\text{m}/\text{ft}^3)$$

... 74

The next component is the friction gradient. For region bubble and slug flow regions, this is determined using the relationship;

$$G_{fr} = 4f_w \frac{V_{sL}^2}{2gd_w}\left(1 + {V_{sg}}/{V_{sL}}\right)$$

... 75

while for mist flow;

$$G_{fr} = 4f_w \frac{\rho_g}{\rho_L}\frac{V_{sg}^2}{2gd_w}$$

... 76

The parameter f_w is determined for bubble and slug flow regions using the following relationship;

$$f_w = \frac{f_1 f_2}{1 + f_1 \sqrt{\frac{V_{sg}}{50 V_{sL}}}}$$

... 77

where the parameters f_1 and f_2 are determined from figures 23 and 24. In mist flow, $f_w = f_1$. The Reynolds number in figure 23 should be that of the liquid phase when in bubble and slug flow regions, and that of the gas phase when in mist flow region.

The final component of the pressure gradient is the acceleration gradient. This is term can be neglected in bubble and slug flow regions but must be included in mist flow region. Assuming isothermal gas expansion, the acceleration gradient is;

$$\left(\frac{dP}{dh}\right)_{ac} = -\left(\rho_L V_{sL} + \rho_g V_{sg}\right)\left(\frac{dV_{sg}}{dh}\right)$$

... 78

but the isothermal gas expansion gives;

$$\frac{d}{dh}\left(P V_{sg}\right) = V_{sg}\frac{dP}{dh} + P\frac{dV_{sg}}{dh} = 0$$

... 79

using equations (79) and (65) gives;

$$G_{ac} = \left(\rho_L V_{sL} + \rho_g V_{sg}\right) V_{sg}\frac{G}{P}$$

... 80

Thus the total pressure gradient is given as follows;

- For bubble and slug flows

$$G = G_{st} + G_{fr}$$

- For mist flow

$$G = \frac{G_{st} + G_{fr}}{1 - \left(\rho_L V_{sL} + \rho_g V_{sg}\right)\left(V_{sg} / P\right)}$$

Note that it will be necessary to adjust the hydrostatic gradient for deviation by multiplying with $\cos\theta$.

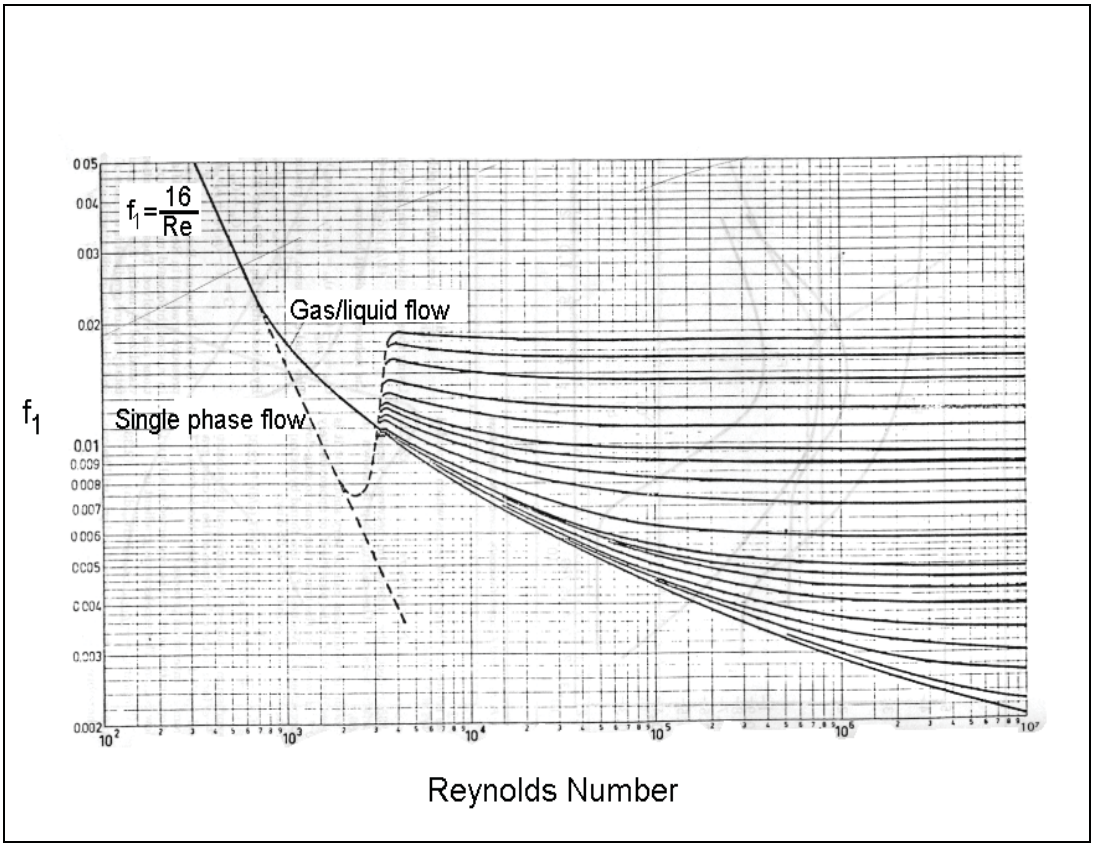

Figure 23: Friction factor, f_1

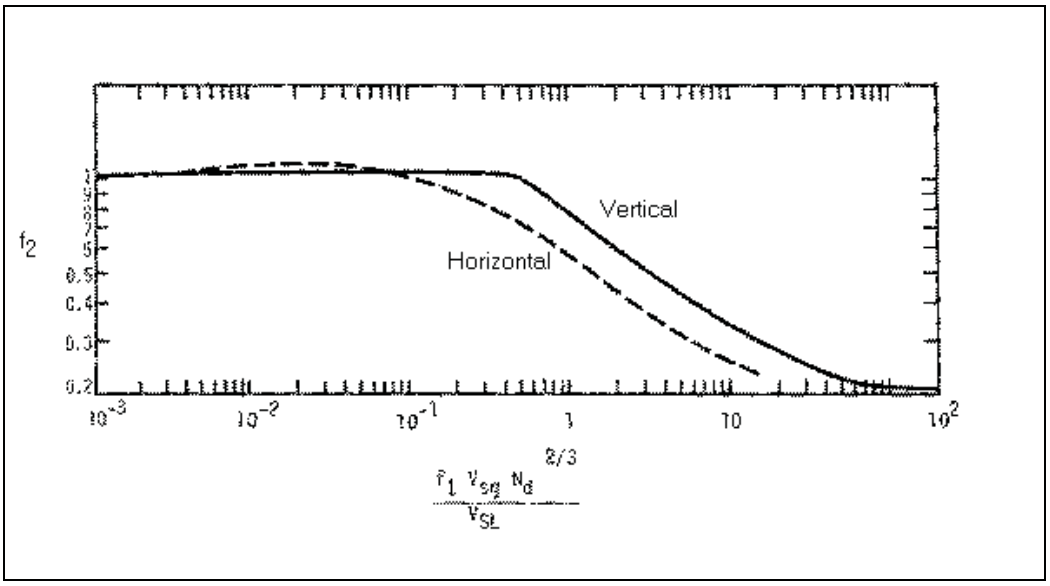

Figure 24: Factor f_2

4.6 Cuttings Transport

Drilling and well cleaning involves the lifting of sand particles and/or drill cuttings. To ensure that the cuttings will be transported to surface, we will need to ensure that the liquid phase velocity, whether in single or multi-phase flow, is greater than the maximum velocity at which the cuttings are falling. This velocity is called the terminal settling velocity and it occurs when equilibrium of the forces acting upon the particle is achieved.

While the shape of these particles may be irregular, we are interested in determining the terminal settling velocity of all shapes. Coincidental, a sphere is the fastest falling object. The following discussion proves that a sphere is the fastest falling object.

Figure 25, shows a particle of ellipsoidal shape. In frame (a) the particle has a high centre of gravity and high potential energy. Stability analysis dictates that any system with high potential energy will be unstable when disturbed by small perturbations, thus will attempt to reduce the potential energy. Frame (b) shows the particle after re-aligning itself to a position with the lowest potential energy. It is clear that the particle in frame (b) will experience more drag than the particle in frame (a). Also, a sphere of equivalent volume will experience less drag than the object in frame (b). Therefore, the sphere will fall faster than the ellipsoidal shape. Thus, we can concentrate our efforts to determine the terminal settling velocity by examining the behaviour of a sphere.

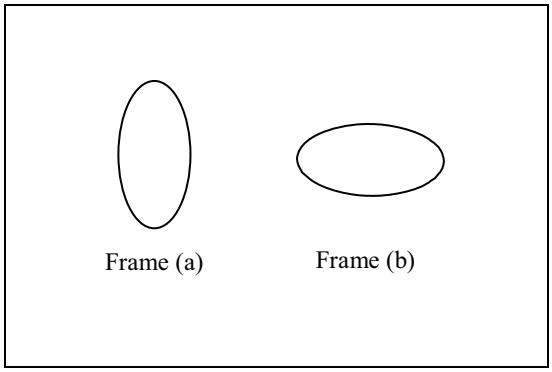

Figure 25: The object in frame (a) is unstable while the object in frame (b) is stable.

G.G.Stokes[6] produced an exact solution for the drag on a sphere falling in an unbounded fluid. The solution neglected the forces of inertia, by setting the Reynolds number to zero (this can be achieved by setting the fluid density to zero). Stokes' solution is valid at very low Reynolds number (≤1). Oseen[7] extended Stokes' solution by including some of the inertia forces (linear momentum in the direction of flow or particle motion). Both solutions give a coefficient of drag, $\boldsymbol{C_D}$;

- Stokes' solution;

$$C_D = \frac{24}{\mathrm{Re}}$$

... 81

- Oseen's solution;

$$C_D = \frac{24}{\mathrm{Re}}\left(1 + \frac{3}{16\,\mathrm{Re}}\right)$$

... 82

Oseen's solution is valid up to $\boldsymbol{Re} \leq 5$. Other formulae for $\boldsymbol{C_D}$ have been established for higher $\boldsymbol{Re}$[8].

- For $\boldsymbol{Re} \leq 500$;

$$C_D = \frac{18.5}{\mathrm{Re}^{0.6}}$$

... 83

- And for $\boldsymbol{Re} > 500$;

$$C_D \approx 0.44$$

... 84

The sphere will reach its terminal settling velocity, $\boldsymbol{V_t}$, when all the forces acting upon it are in equilibrium. These forces include weight, $\boldsymbol{W}$, buoyancy, $\boldsymbol{B}$, and drag, $\boldsymbol{D}$;

$$W - B = D$$

... 85

or;

$$\frac{4\pi}{3}\left(\frac{d}{2}\right)^3 g(\rho_P - \rho\ ) = \frac{1}{2} C_D \rho\ V_t^2 \pi \left(\frac{d}{2}\right)^2$$

... 86

where $\boldsymbol{\rho_p}$ is the particle density. Substituting equation (81) in (86) gives;

$$V_t = \frac{d^2 g(\rho_P - \rho\ )}{18\eta}$$

... 87

and substituting (83) in (86) gives;

$$V_t = e^{\frac{\log\{\frac{4d^{1.6}g(\rho_P - \rho\ )}{55.5\rho^{0.4}\eta^{0.6}}\}}{1.4}}$$

... 88

and substituting (84) in (86) gives;

$$V_t = \sqrt{3.03dg\left(\frac{\rho_P - \rho}{\rho}\right)}$$

... 89

The range of validity being ***Re***≤1 for equation (87), ***Re***≤500 for equation (88), and ***Re***>500 for equation (89).

Note that the discussion above applies to the particle Reynolds number. The fluid viscosity that should be used is the effective viscosity, which can be derived from the flow conditions. Also, this analysis is based on vertical flow, thus the terminal velocity is normally multiplied by a factor of up to 10 to allow for high deviations.

4.7 Maximum Penetration Rate

Experimental evidence has shown that cuttings can only be transported if no congestion of particles occurs[9]. When congestion does occur, the particles in the shadow of lower particles will experience less drag thus will fall faster. This process continues until a certain or critical concentration by volume is reached. The critical concentration by volume was determined experimentally for oil field applications at about 5% (corresponds to about 1 lbs of sand per 1 gal of water).

The maximum penetration rate must not exceed the rate at which the cuttings are being transported to surface. That is, the volumetric cuttings rate is a maximum of 5% times the liquid phase flow rate. When this is translated to velocity, it will be the maximum penetration rate. Normally, in drilling applications, a lower concentration by volume of about 2-3% is used.

4.8 Under-Balanced Drilling

One of the main advantages of using coiled tubing for drilling is that well control and fluid circulation can be maintained at all times. Thus the pressure in the borehole does not have to exceed the formation pressure to avoid accidents. When the pressure in the borehole is lower than the pressure in the formation, particularly opposite the reservoir, the drilling operation is said to be under-balanced.

Under-balanced drilling conditions have their own advantages over over-balanced drilling conditions. The main advantages being that no invasion of the reservoir takes place, which also means no skin damage, and if the reservoir has reasonably good permeability then production could take place simultaneously as drilling. If indeed production does take place then this will assist in the carrying of cuttings to surface.

An under-balanced drilling condition is achieved by reducing the effective density of the fluids in the well. One method will be to use a lighter fluid such as diesel or oil based mud. If this is not sufficient or not feasible because of environmental concerns, then nitrogen gas is injected to produce multi-phase flow or foam. In gas producing wells, the gases from the reservoir could assist in reducing the effective fluid density, thus the nitrogen requirements may be reduced or even made redundant after production is initiated. To be able to ascertain that under-balanced drilling conditions are attained, the algorithms described above must be used to determine the optimum fluid and gas rates together with any production from the reservoir.

4.9 Reservoir Production

Reservoir production is only possible to include in the fluid circulation if some inflow performance of the reservoir is already known. This is normally made available from neighbouring wells, or if the well being drilled is a development well, then the chances are that the reservoir properties are already known.

Several mathematical models have been suggested for modelling the reservoir production[5]. A linear method, using a parameter known as the productivity index, ***PI***, suggests that the production, $\boldsymbol{Q_{res}}$, is directly proportional to the difference between the static reservoir pressure, $\boldsymbol{P_{res}}$, and the flowing bottom hole pressure, $\boldsymbol{P_{BHFP}}$;

$$Q_{res} = PI(P_{res} - P_{BHFP})$$

... 90

Using the productivity index method requires knowledge of one inflow performance. Another more realistic relationship was suggested by Fetkovitch[10] and requires knowledge of at least two inflow performances to compute the necessary parameters, ***C*** and ***n***;

$$Q_{res} = C\left(P_{res}^2 - P_{BHFP}^2\right)^n$$

... 91

The above relationships are concerned with one of the phases of the reservoir production, normally the liquid phase. A gas to oil ratio, ***GOR***, is also used to compute the gas flow rate, and is considered a constant regardless of the oil flow rate. If the reservoir is producing gas only, then equations (90) and (91) will be adapted to compute the gas flow rate.

4.10 Nomenclature

B	Buoyancy (on a sphere)
B_{gas}	Gas volume factor
C	Constant in Fetkovitch reservoir production model
C_D	Coefficient of drag (on a sphere)
D	Fluid drag (on a sphere)
d	Pipe (or coiled tubing) inner diameter
d_c	Coiled tubing outer diameter
d_o	Wellbore inner diameter (or diameter of outer pipe in annular flow)
d_w	Effective flow domain diameter
f	Friction factor
G	Non-dimensional pressure gradient
g	Acceleration due to gravity
H_L	Liquid holdup
h	Height
K	Consistency factor for Power-Law fluids
n	Power index for Power-Law fluids, power index for Fetkovitch reservoir production model
P	Fluid pressure
P_{dyn}	Dynamic fluid pressure
P_{hyd}	Hydrostatic fluid pressure
PI	Reservoir productivity index
PV	Plastic viscosity for Bingham-Plastic fluids
Re	Reynolds number, representative of inertia to viscous forces
S	Slip factor
T	Absolute temperature
tvd	True vertical depth
Q	Volumetric flow rate
Q_{res}	Reservoir production flow rate
V	Fluid velocity
V_S	Slip velocity
V_{sg}	Superficial gas velocity
V_{sL}	Superficial liquid velocity
V_t	Terminal settling velocity (of a sphere)
W	Weight (of a sphere)
YP	Yield point for Bingham-Plastic fluids

z	Gas compressibility factor
γ	Shear rate
γ_g	Gas specific gravity, relative to air at standard pressure and temperature
η	Fluid viscosity
θ	Well deviation
ρ	Fluid density
ρ_g	Gas density
ρ_L	Liquid phase density
ρ_P	Particle density (of a sphere)
σ	Fluid surface tension
τ	Shear stress

4.11 References

1. Massey, B.S. "Mechanics of Fluids", 3rd edition 1975, Van Nostrand Reinhold Publication.
2. International Drilling Fluids (IDF), Technical Manual.
3. Bruce H. Sage and William N. Lacey, Monograph on API Research Project #37 "Thermodynamic Properties of the Lighter Paraffin Hydrocarbons and Nitrogen" American Petroleum Institute Publication, 1950.
4. Blauer, R.E., Mitchell, B.J., and Kohlhaas, C.A. "Determination of Laminar, Turbulent, and Transitional Foam Flow Losses in Pipes", SPE paper no.4885, 1974.
5. Kermit E.Brown and H.Dale Beggs "The Technology of Artificial Lift Methods", Vol. I, PennWell Books Publication, 1977.
6. Stokes, G.G. 1851 Trans. Camb. Phil. Soc. 9, 8. (Mathematical and Physical Papers 3, 1).
7. Oseen, C.W. 1910 Ark. f. Mat. Astr. Og Fys. 6, no. 29.
8. Sas-Jaworsky II, Alexander "Coiled Tubing … Operations and Services, Part 4 - Sand and Solids Washing", World Oil, Mar. 1992.
9. Ziedler, Ph.D. Thesis, University of Tulsa, Oklahoma, 1973.
10. Fetkovitch, M.J. "The Isochronal Testing of Oil Wells", SPE paper no. 4529, 48th Annual Fall Meeting of SPE of AIME, Las Vegas, Sep.-Oct. 1973.

Appendix

Example 1

This example illustrates the effect of the stability criterion on the coiled tubing lockup. The proposed drilling is not feasible with the 2" coiled tubing string. Several scenarios have been attempted utilising different BHAs to try and vary the stability of the coiled tubing, but with no success. One scenario that will actually get the coiled tubing into the well is to use a back pressure valve pre-set at 5.6 MPa. However, when at T.D. and drilling is commenced the fluid circulation pressures will be too high and the stability of the coiled tubing will revert to unstable thus making the coiled tubing drilling job non-feasible because of lack of WOB.

Input Data Summary

Coiled Tubing

2" x 0.125", minimum yield 80,000 psi, total length 3500 m.

Existing Completion/Open Hole Geometry

8 1/2" x 35.71 lbs/ft to depth 126 m.
5 1/2" x 20.83 lbs/ft to depth 646 m.
4 1/2" x 20.09 lbs/ft to depth 2105 m.

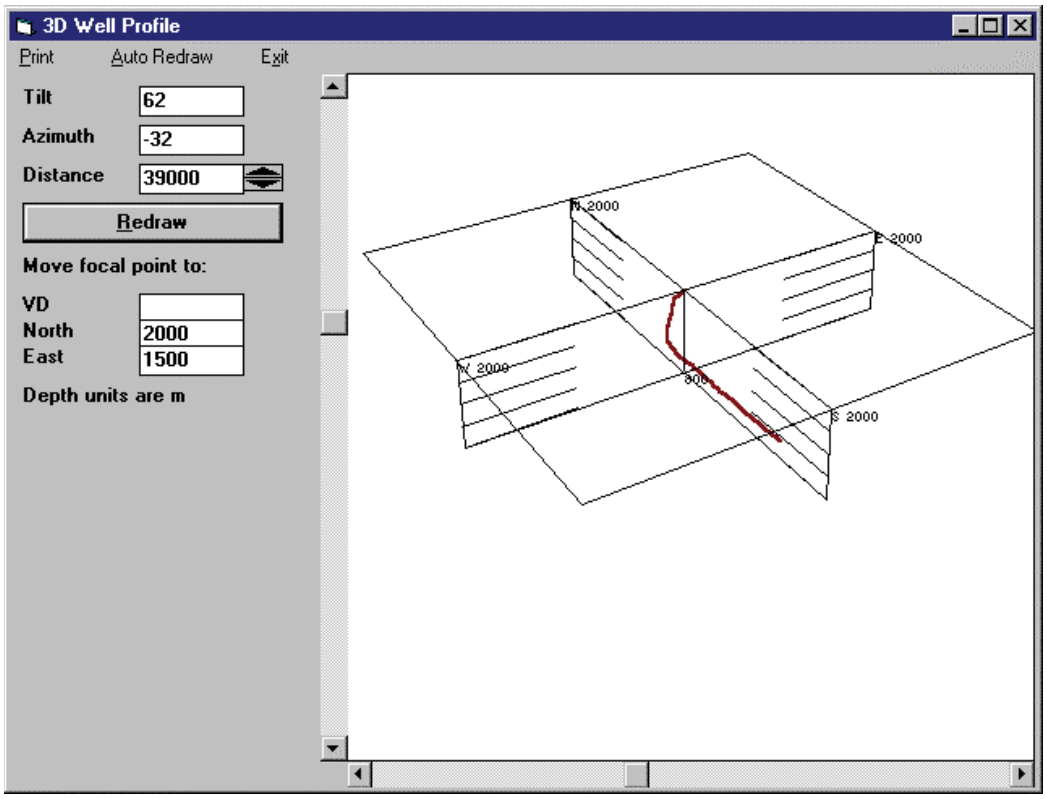

The well profile in 3D

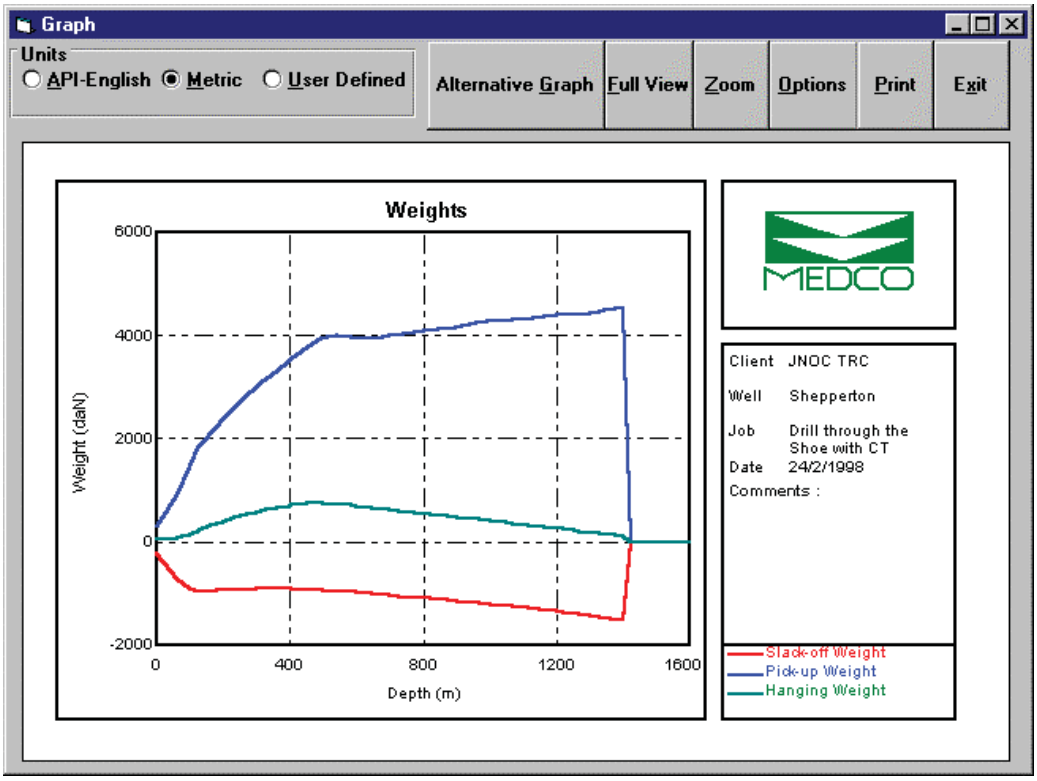

Weight results showing lockup at 1423 m.

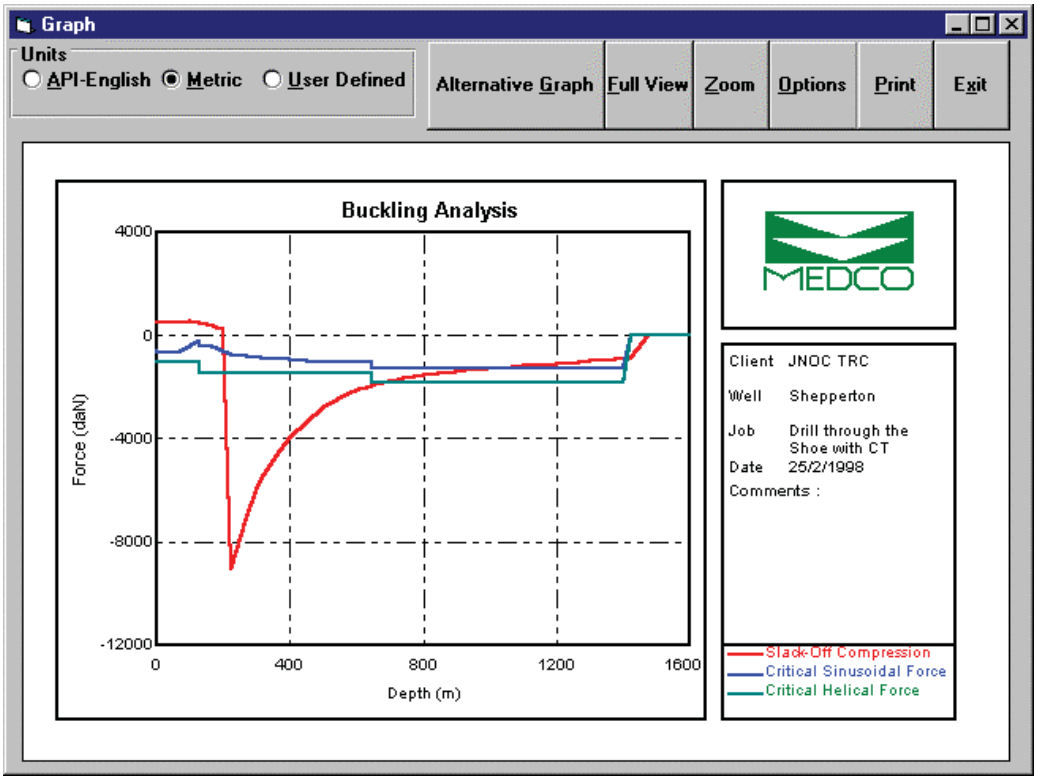

Helical buckling starting from 700 m upwards and lockup at 225 m

Example 2

This example shows the WOB that could be achieved in an under-balanced coiled tubing drilling job. A high penetration rate is possible with this job. Also, this example illustrates the use of nitrified fluids to achieve an under-balanced condition. The total flow in the annulus assists in cuttings transport.

Input Data Summary

Coiled Tubing

3 1/2" x 0.224", minimum yield 70,000 psi, total length 5123 m.

Existing Completion/Open Hole Geometry

5 1/2" x 20.83 lbs/ft to depth 1079 m.

4 3/4" open hole to depth 1453 m.

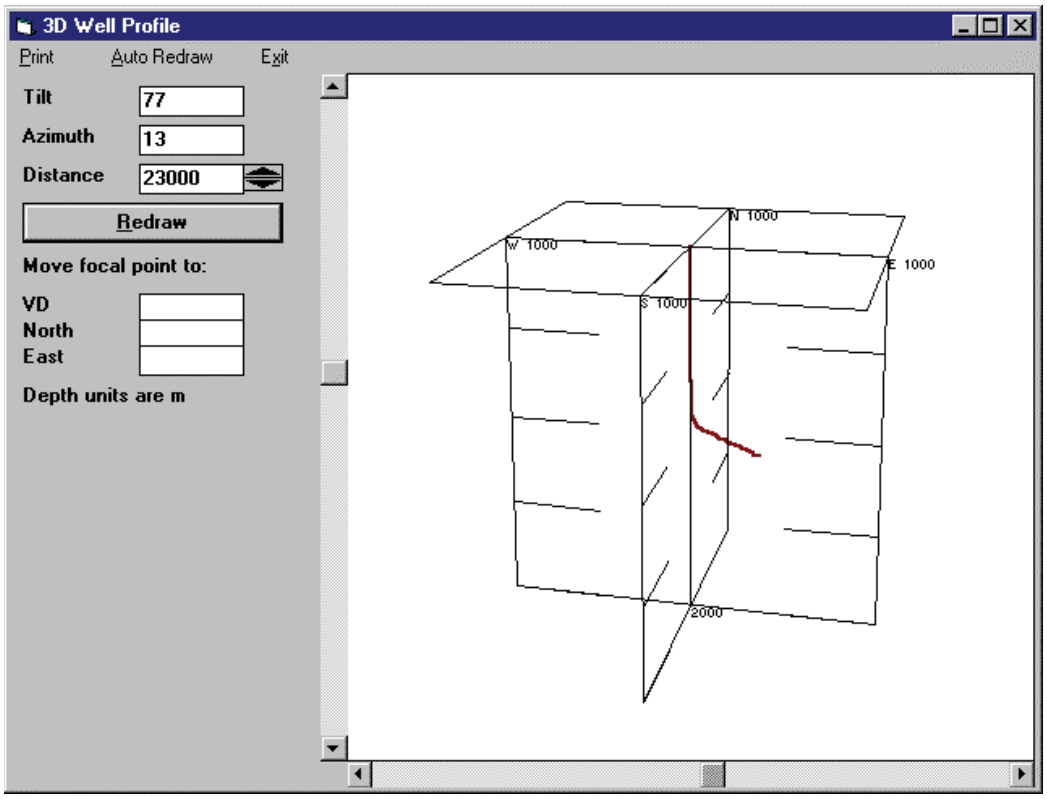

3D Well Profile

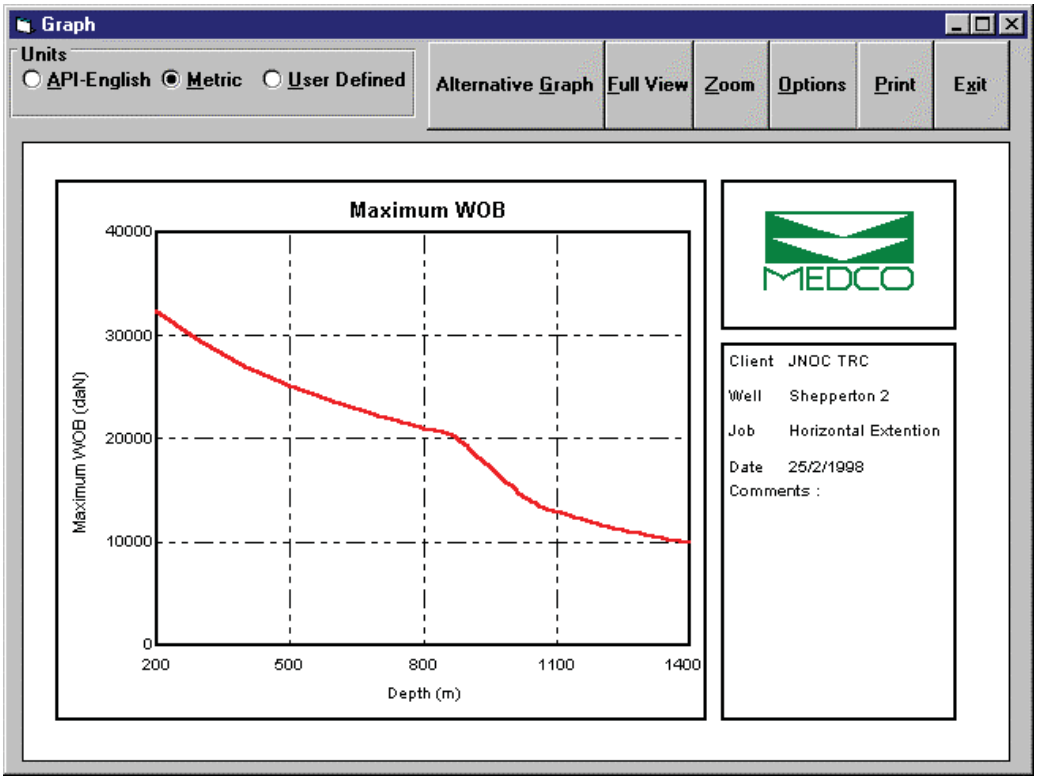

Maximum Weight-on-Bit

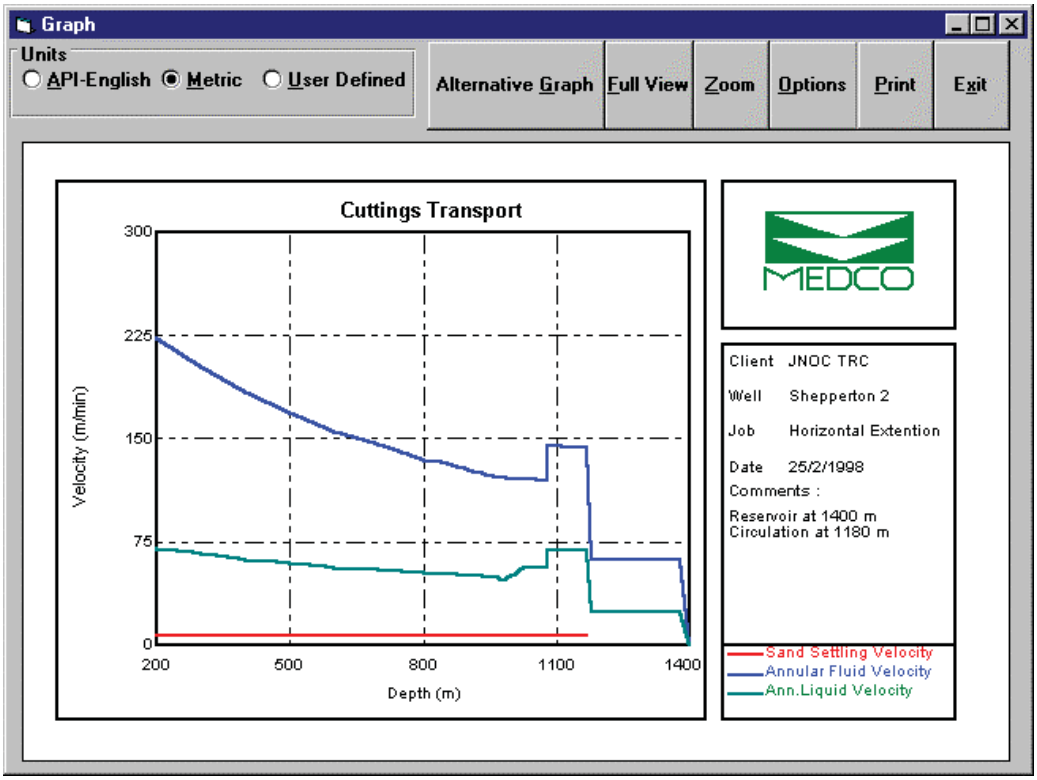

Settling velocity well below annular liquid velocity throughout the well

Parameter Name	Flow Type	Fluid Type		
		Newtonian	Power Law	Bingham Plastic
Velocity Q in gal/min V in ft/sec d in inches	Pipe	$V = \frac{Q}{2.448d^2}$		
	Annular	$V = \frac{Q}{2.448\left(d_2^2 - d_1^2\right)}$		
Reynolds Number ρ in ppg μ in cps	Pipe	$N_{\mathrm{Re}} = \frac{928\rho V d}{\mu}$	$N_{\mathrm{Re}} = \frac{89100\rho V^{2-n}}{K}\left(\frac{0.0416d}{3+1/n}\right)^n$	$N_{\mathrm{Re}} = \frac{928\rho V d}{\mu_P}$
	Annular	$N_{\mathrm{Re}} = \frac{757\rho V(d_2 - d_1)}{\mu}$	$N_{\mathrm{Re}} = \frac{109000\rho V^{2-n}}{K}\left[\frac{0.0208(d_2 - d_1)}{2+1/n}\right]^n$	$N_{\mathrm{Re}} = \frac{757\rho V(d_2 - d_1)}{\mu_P}$
Hedstrom Number	Pipe			$N_{He} = \frac{37100\rho\tau_Y d^2}{\mu_P^2}$
	Annular			$N_{He} = \frac{24700\rho\tau_Y (d_2 - d_1)^2}{\mu_P^2}$
Critical Reynolds Number	Pipe & Annular	$N_{\mathrm{Re}} = 2100$	$n < 0.2; N_{\mathrm{Re}} = 4200$ $0.2 < n \le 0.45; N_{\mathrm{Re}} = 5960 - 8800n$ $n > 0.45; N_{\mathrm{Re}} = 2000$	$N_{\mathrm{Re}} = 1798.64 - 0.00201815N_{He}$ $+ 15.7373\sqrt{N_{He}} + 3.73074 * 10^{-11} N_{He}^2$
Laminar Pressure Loss Per	Pipe	$\Delta P = \frac{\mu V}{1500d^2}$	$\Delta P = \frac{KV^n(\frac{3+1/n}{0.0416})^n}{144000d^{n+1}}$	$\Delta P = \frac{\mu_P V}{1500d^2} + \frac{\tau_Y}{225d}$

Unit Length **ΔP in psi**	**Annular**	$\Delta P = \frac{\mu V}{1000(d_2 - d_1)^2}$	$\Delta P = \frac{KV^n(\frac{2+1/n}{0.0208})^n}{144000(d_2 - d_1)^{n+1}}$	$\Delta P = \frac{\mu_P V}{1000(d_2 - d_1)^2} + \frac{\tau_Y}{200(d_2 - d_1)}$
Turbulent Pressure Loss Per Unit Length	**Pipe**	$\Delta P = \frac{f\rho V^2}{25.8d}$		
	Annular	$\Delta P = \frac{f\rho V^2}{21.1(d_2 - d_1)}$	$\frac{1}{\sqrt{f}} = -4\log\left\{0.269\frac{\varepsilon}{d} + \frac{1.255}{\mathrm{Re}\sqrt{f}}\right\}$	